© 2021. Published by The Company of Biologists Ltd | Journal of Cell Science (2021) 134, jcs250191. doi:10.1242/jcs.250191

RESEARCH ARTICLE

Sequestration of the PKC ortholog Pck2 in stress granules as a feedback mechanism of MAPK signaling in fission yeast

Yuki Kanda[1], Ryosuke Satoh[1], Teruaki Takasaki[1], Naofumi Tomimoto[1], Kiko Tsuchiya[1], Chun An Tsai[1], Taemi Tanaka[1], Shu Kyomoto[1], Kozo Hamada[1], Toshinobu Fujiwara[2] and Reiko Sugiura[1,*]

ABSTRACT

Protein kinase C (PKC) signaling is a highly conserved signaling module that plays a central role in a myriad of physiological processes, ranging from cell proliferation to cell death, via various signaling pathways, including MAPK signaling. Stress granules (SGs) are non-membranous cytoplasmic foci that aggregate in cells exposed to environmental stresses. Here, we explored the role of SGs in PKC/MAPK signaling activation in fission yeast. High-heat stress (HHS) induced Pmk1 MAPK activation and Pck2 translocation from the cell tips into poly(A)-binding protein (Pabp)-positive SGs. Pck2 dispersal from the cell tips required Pck2 kinase activity, and constitutively active Pck2 exhibited increased translocation to SGs. Importantly, Pmk1 deletion impaired Pck2 recruitment to SGs, indicating that MAPK activation stimulates Pck2 SG translocation. Consistently, HHS-induced SGs delayed Pck2 relocalization at the cell tips, thereby blocking subsequent Pmk1 reactivation after recovery from HHS. HHS partitioned Pck2 into the Pabp-positive SG-containing fraction, which resulted in reduced Pck2 abundance and kinase activity in the soluble fraction. Taken together, these results indicate that MAPK-dependent Pck2 SG recruitment serves as a feedback mechanism to intercept PKC/MAPK activation induced by HHS, which might underlie PKC-related diseases.

KEY WORDS: PKC, Stress granules, MAPK signaling, Spatiotemporal regulation, Heat stress, Phase separation

INTRODUCTION

The protein kinase C (PKC) family is a member of the AGC kinase superfamily of serine/threonine protein kinases that play essential roles in cell growth and cell death (Newton, 2010) by transmitting extracellular signals to various downstream signaling pathways, including MAPK. In mammalian systems, the PKC–Raf–MEK–ERK signaling pathway modulates gene expression and cell proliferation in various cell types, including endothelial cells, T-cells and various cancer cell settings (Pintus et al., 2003; Hoyer et al., 2005; Li et al., 2012). Despite the importance of PKC signaling deterioration in various diseases, including cancers and neurodegenerative disorders such as Alzheimer's disease, how PKC regulates these pathophysiological roles remains obscure (Lucke-Wold et al., 2015; Callender and Newton, 2017; Isakov, 2018).

[1]Laboratory of Molecular Pharmacogenomics, Department of Pharmaceutical Sciences, Faculty of Pharmacy, Kindai University, Osaka 577-8502, Japan. [2]Laboratory of Biochemistry, Department of Pharmacy, Faculty of Pharmacy, Kindai University, Osaka 577-8502, Japan.

*Author for correspondence (sugiurar@phar.kindai.ac.jp)

R.S., 0000-0001-6946-0935

Handling Editor: John Heath
Received 16 June 2020; Accepted 23 November 2020

A similar PKC-dependent regulation of the MAPK signal transduction pathway has been described in both budding and fission yeasts. The yeast *Saccharomyces cerevisiae* produces only a single Pkc1, whereas the fission yeast *Schizosaccharomyces pombe* has two PKC homologs, Pck1 and Pck2 (Arellano et al., 1999; Fuchs and Mylonakis, 2009). In fission yeast, Pck2 is a primary upstream activator of the cell integrity MAPK signaling pathway, composed of a three-tiered Mkh1–Pek1–Pmk1 kinase cascade (Toda et al., 1996; Ma et al., 2006). Rho small GTPases, as well as PDK1 homologs, participate in the activation of PKC in both yeasts by mechanisms involving protein–protein interaction via the HR1 Rho-binding domains (Sayers et al., 2000) and phosphorylation at the activation loop (Madrid et al., 2015), respectively. Thus, conservation between the fission yeast Pcks and the mammalian PKN1/2 [also known as protein kinase C-related protein kinase (PRK)1/2] (Mukai, 2003) may exist at structural and regulatory levels (Sayers, et al., 2000).

Importantly, the biological activity of PKC enzymes is tightly regulated by their subcellular localization (Newton and Jhonson, 1998; Gould and Newton, 2008), as exemplified by PKC translocation to the plasma membrane in response to various stimuli. Recently, a research group demonstrated that PKC alpha (also known as PRKCA) in mammals localizes to stress granules (SGs) upon heat stress (HS) (Kobayashi et al., 2012), but the function and mechanism of PKC SG localization remain unclear. SGs are non-membranous cytoplasmic foci, composed of non-translating messenger ribonucleoproteins that rapidly aggregate in cells exposed to a variety of environmental stresses, including oxidative, hyperosmotic or heat stresses (Guil et al., 2006; Anderson and Kedersha, 2006, 2009). Representative components of SGs include poly(A)-binding protein (PABP; also known as PABPC1), translation factors such as eIF3 (also known as EIF3A), eIF4E and eIF4G (also known as EIF4G1), as well as specific RNA-binding proteins (RBPs), such as TIA-1 and TIAR (also known as TIAL1) (Panas et al., 2016). Notably, many signaling molecules, such as mTOR, RACK1 and calcineurin, are recruited to SGs, thereby constituting signaling hubs that can rewire signal transduction (Thedieck et al., 2013; Wippich et al., 2013; Arimoto et al., 2008; Higa et al., 2015). Despite recent progress in understanding the repertoires of signaling molecules contained in SGs, little is known about the mechanism or the physiological significance of PKC SG recruitment.

We have previously established molecular genetic screens for negative regulators of PKC-mediated Pmk1 MAPK signaling in fission yeast (Sugiura et al., 1998; Ma et al., 2006). The rationale for this screen relies on the finding that hyperactivation of Pmk1 MAPK signaling is toxic under some conditions, including Pck2 overexpression. We then isolated multi-copy suppressors of the MAPK hyperactivation-dependent cytotoxicity induced by Pck2 overexpression. We identified the dual-specificity phosphatase Pmp1; PP2C phosphatases Ptc1 and Ptc3, which inactivate Pmk1

Journal of Cell Science (2021) 134, jcs250191. doi:10.1242/jcs.250191

MAPK; the SH3-adaptor protein Skb5, which spatially regulates Mkh1 MAPKKK (Sugiura et al., 1998; Takada et al., 2007; Kanda et al., 2016); and Ded1. Ded1 is similar to mammalian DDX3 (also known as DDX3X) and belongs to the highly conserved DEAD-box ATPases that are representative components of SGs (Grallert et al., 2000; Hilliker et al., 2011). Given the isolation of the SG-resident protein Ded1 as a negative regulator of PKC/MAPK signaling, together with the finding that PKC in mammals translocates to SGs, we hypothesized that SGs might be functionally relevant to repress Pck2-mediated MAPK signaling activation.

In this study, we explored the role of SGs in PKC/MAPK signaling activation in fission yeast. Heat stress at 45°C [high-heat stress (HHS)] induced both MAPK hyperactivation and a dynamic change in Pck2 intracellular localization from the plasma membrane, particularly enriched at the growing cell tips (hereafter referred to as 'cell tips'), to the SGs. We show that Pck2 needs its kinase activity for its dispersal from the cell tips and subsequent recruitment into SGs. Notably, Pmk1 MAPK activity is a key determinant of Pck2 translocation into SGs, as MAPK signaling disruption limits Pck2 translocation into SGs. Consequently, Pck2, when localized at SGs, failed to reactivate MAPK signaling after HHS recovery. Intriguingly, HS at 45°C (i.e. HHS), but not at 43°C, preferentially partitioned Pck2 into SGs, thereby reducing Pck2 kinase activity in the soluble fraction. Taken together, these findings indicate a role for SGs as signaling hubs to intercept PKC/MAPK signaling activation upon HHS by spatial PKC sequestration. Failure to coordinate this 'feedback circuit' might lead to vulnerability to various PKC-regulated diseases, including cancer.

RESULTS

HS induces Pck2 translocation into SGs

As a first step to investigate the functional connection between SGs and PKC-mediated MAPK signaling, we analyzed the effect of HS, a physiological SG-inducing stimulus, on the subcellular localization of Pck2. For this purpose, the endogenous Pck2 protein tagged with GFP (Pck2-GFP) was visualized, and the effect of HS was analyzed. Under the unstressed condition, fluorescence of the endogenous Pck2-GFP was mainly localized to the cell tips, as previously reported (Fig. 1A, 0 min, arrowheads) (Kanda et al., 2016). Upon HS (45°C), Pck2-GFP underwent dynamic changes in its intracellular localization from the cell tips to the dot-like structures (Fig. 1A, 20 min, 60 min, arrows). Quantification of the number of cells harboring the cell tip-localized Pck2 showed that HS induced Pck2 dispersal from the cell tips within 5 min after HS exposure (Fig. 1B, top, 5 min). By contrast, the number of Pck2 dots increased during HS (Fig. 1B, bottom). In mammalian cells and budding and fission yeasts, Pabp is a representative SG marker, and is routinely used to study SG dynamics in live cells (Kedersha and Anderson, 2007; Nilsson and Sunnerhagen, 2011; Brambilla et al., 2017). We, therefore, co-expressed Pabp tagged with tdTomato expressed from the endogenous loci to examine its colocalization with Pck2. The results showed that the Pck2-GFP dots colocalized with the Pabp-tdTomato dots upon HS (Fig. 1A), suggesting that Pck2 translocated into SGs upon HS. The number of Pabp dots also increased during HS, showing that Pck2 and Pabp displayed similar kinetics in terms of their translocation to dot-like structures upon HS. Quantification showed that approximately half of the Pck2 dots colocalized with Pabp dots (Fig. 1B, bottom). We also observed the colocalization of fluorescence of Pck2-GFP and tdTomato-fused Nrd1, which also serves as a representative SG-resident protein (Satoh et al., 2012), co-expressed from their endogenous loci upon HS, and, similar to Pabp, approximately half of the Pck2 dots colocalized with Nrd1 dots, further supporting the idea that Pck2 was recruited to SGs upon HS (Fig. 1C,D).

Cycloheximide (CHX) is known to be a potent inhibitor of SG formation (Kedersha et al., 2000; Mazroui et al., 2002; Mollet et al., 2008). We, therefore, used CHX to prevent SG formation and examined the impact of the inhibition of SG formation on Pck2-GFP localization (Fig. 1E). CHX treatment markedly inhibited the formation of SGs as judged by the decreased number of Pabp dots (Fig. 1F, bottom). The formation of Pck2-GFP dots under HS was also significantly inhibited by CHX treatment (Fig. 1F, top), suggesting that the formation of Pck2-GFP dots upon HS is dependent on SG formation.

Pck2 translocates into SGs in a Pck2 kinase-dependent manner

What is the regulatory mechanism to stimulate Pck2 SG translocation? To investigate how Pck2 is recruited into SGs, we tested whether the kinase activity of Pck2 was required for its localization upon HS. For this, we created cells expressing the genomic version of the kinase-negative mutant Pck2 protein tagged with GFP (Pck2 K712W-GFP) under its native promoter (Fig. 2A). To gain a precise understanding of the impact of Pck2 kinase activity on the subcellular distribution of Pck2, we also created cells expressing the genomic version of the constitutively active mutant allele of Pck2, encoding Ala instead of Arg389 (Pck2 R389A) at the pseudo-substrate domain (Fig. 2A) (Watanabe et al., 1994).

To directly assess the *in vitro* kinase activity of these mutant Pck2 proteins compared with the wild-type (WT) Pck2, we used the PepTag system (Sukumaran and Prasadarao, 2002; Shao and Bayraktutan, 2013). The phosphorylated peptide (phosphorylated bands) migrates towards the positive electrode, whereas the non-phosphorylated peptide (non-phosphorylated bands) migrates towards the negative electrode. We first validated whether fission yeast Pck2 kinase activity can be measured using the PepTag system, and GST-Pck2, but not GST protein, expressed and purified from fission yeast was shown to induce the mobility shift of the phosphorylated peptide, which also appeared with the addition of mammalian PKC as a positive control (Fig. S1).

We then compared the kinase activity of the cells expressing WT Pck2 (Pck2 WT-GFP), kinase-negative Pck2 (Pck2 K712W-GFP) or constitutively active Pck2 (Pck2 R389A-GFP) from the endogenous promoter. These Pck2-GFP proteins were expressed at similar levels, as shown by the analysis of whole-cell lysates blotted with anti-GFP antibodies (Fig. 2B,C). The kinase-negative Pck2 protein immunoprecipitated from the lysates of the mutant strain exhibited markedly reduced kinase activity against substrates compared with Pck2 WT (Fig. 2B). By contrast, the kinase activity of the constitutively active Pck2 R389A was significantly higher than that of the Pck2 WT kinase (Fig. 2C).

We then visualized the subcellular localization of the cells harboring the genomic version of Pck2 K712W-GFP and Pck2 R389A-GFP upon HS. Pck2 K712W-GFP localized at the cell tips in unstressed cells (Fig. 2D, 0 min). Notably, upon HS, the number of dots expressing the Pck2 K712W-GFP mutant protein was markedly lower (~30% of that of Pck2 WT-GFP), and a significantly higher number (~40%) of cells expressing Pck2 K712W maintained cell tip localization even after 60 min (Fig. 2D,E). Thus, Pck2 kinase activity is required for the dispersal of Pck2 from the cell tips and subsequent SG localization.

To evaluate the constitutively active nature of Pck2 R389A, we incubated the cells at a lower temperature of 44°C, because HS at 45°C (HHS) did not discriminate between Pck2 WT-GFP and Pck2 R389A-GFP in terms of their subcellular distribution at the SGs (Fig. S2). Upon HS at 44°C, the numbers of Pck2 dots and Pabp

Journal of Cell Science (2021) 134, jcs250191. doi:10.1242/jcs.250191

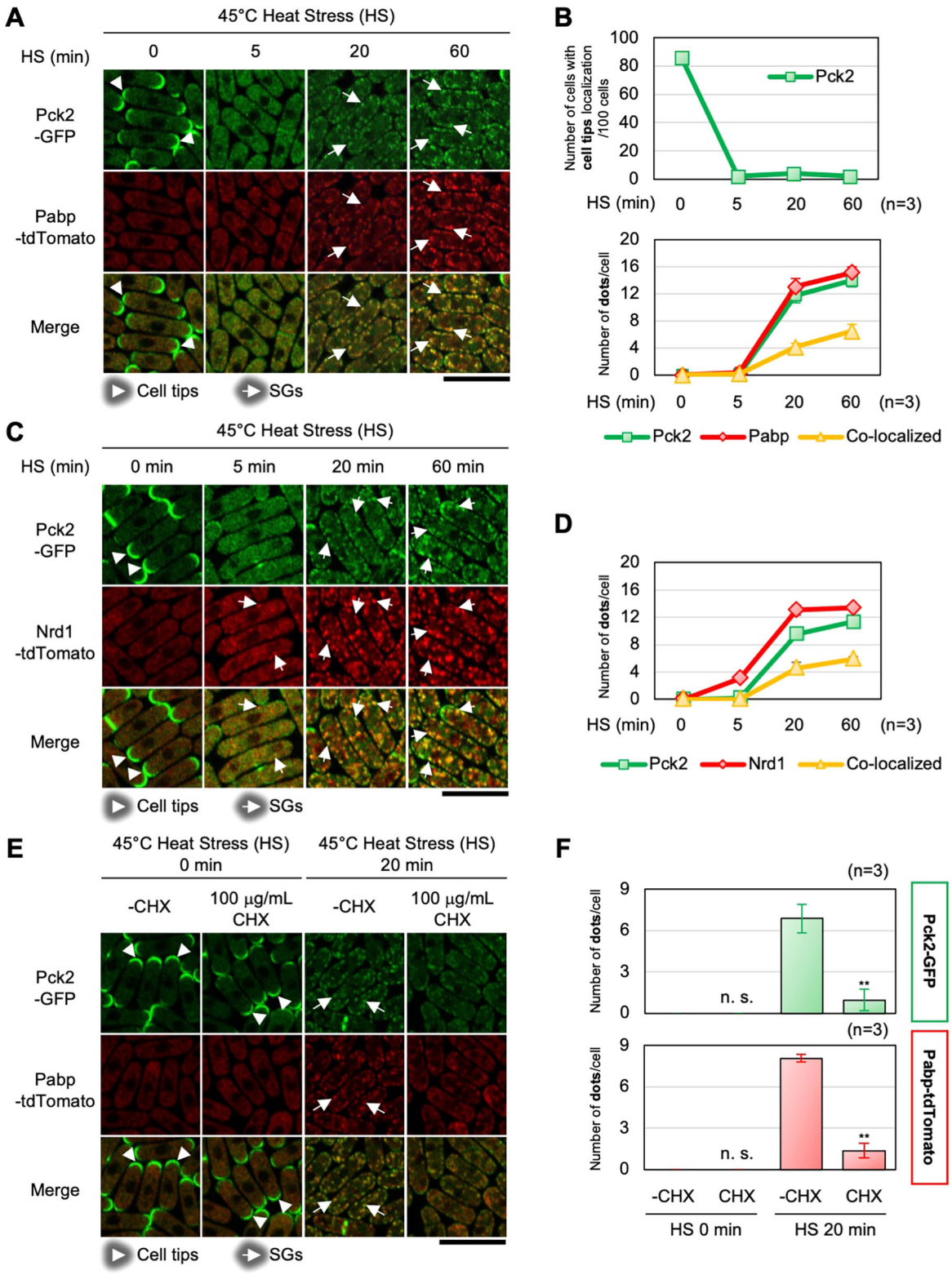

Fig. 1. See next page for legend.

dots were ~50% (three to six/cell) of those at 45°C (ten to 12/cell) (Fig. 2F; Fig. S3B). The number of Pck2 R389A-GFP dots upon HS (44°C) was almost 2.5-fold (eight/cell) of that of Pck2 WT-GFP (three/cell) upon HS for 60 min (Fig. 2F,G). Notably, cells harboring the Pck2 WT-GFP recovered their cell tip localization 60 min after the HS (44°C), whereas Pck2 R389A dispersed from the cell tips but failed to relocalize to the cell tips; instead, it largely translocated to the SGs (Fig. 2F,G, 60 min). Thus, in contrast to the kinase-negative Pck2, Pck2 R389A displayed higher SG localization and sustained dispersal from the cell tips, further supporting the possibility that Pck2 translocates into SGs in a kinase-dependent manner.

Journal of Cell Science (2021) 134, jcs250191. doi:10.1242/jcs.250191

Fig. 1. Heat stress (HS) causes Pck2 translocation from the cell tips to the stress granules (SGs). (A) Pck2 undergoes dynamic changes in its subcellular distribution upon HS. Wild-type cells expressing Pck2-GFP and Pabp-tdTomato were grown in EMM at 27°C for 20 h, then localization of Pck2-GFP and Pabp-tdTomato was observed before (0 min) and after a shift to 45°C for 5, 20 and 60 min. Arrowheads and arrows indicate the representative cell tip localization and foci, respectively, in which Pck2-GFP (green) colocalized with Pabp-tdTomato (red). (B) The number of cells harboring the cell tip-localized Pck2 per 100 cells (top), the numbers of dots of Pck2 or Pabp per cell, and the number of Pck2 dots colocalizing with Pabp (bottom) at the indicated time points after HS were shown. Graphs show the mean±s.d. (n=3). (C) HS induced Pck2 translocation into Nrd1-positive SGs. Pck2-GFP was observed in living cells grown at 27°C (0 min) after a shift to 45°C for 5, 20 and 60 min. Arrowheads indicate the cell tip localization. Arrows indicate representative foci in which Pck2-GFP (green) colocalized with Nrd1-tdTomato (red) after a shift to 45°C for 20 min and 60 min. (D) The number of cells harboring the cell tip-localized Pck2 per 100 cells (top), the numbers of dots of Pck2 or Nrd1 per cell, and the number of Pck2 dots colocalizing with Nrd1 (bottom) at the indicated time points after HS are shown. Graphs show the mean±s.d. (n=3). (E) Wild-type cells expressing Pck2-GFP and Pabp-tdTomato were pre-incubated with or without cycloheximide (CHX) at 27°C for 2 min, then observed before (0 min) and after a shift to 45°C for 20 min. (F) The numbers of Pck2 and Pabp dots per cell at each condition are shown. Graphs show mean±s.d. (n=3). **P<0.01; n.s., not significant; significantly different from control by paired Student's t-test; see Materials and Methods. Scale bars: 10 µm.

It should be noted that the cells expressing Pck2 K712W-GFP or Pck2 R389A-GFP were able to form SGs upon HS as efficiently as the cells harboring Pck2 WT, as judged by the number of Pabp dots during HS, indicating that Pck2 kinase activity does not affect the SG assembly process (Fig. S3A,B).

To investigate whether the active Pck2 preferentially locates to SGs, we undertook experiments to visualize both active and inactive Pck2 fused to a distinct fluorescent tag. For this, we visualized the endogenous kinase-dead (inactive) Pck2 K712W-GFP and investigated the effect of exogenous expression of the constitutively active version of Pck2 R389A fused to mCherry. In addition, the endogenously expressed active Pck2 R389A-GFP was visualized and the effect of exogenous expression of inactive mCherry-Pck2 K712W was investigated. The results showed that inactive Pck2 K712W-GFP was observed to persist in the plasma membrane and translocated to SGs to a lesser extent compared with the exogenously expressed mCherry-Pck2 R389A (Fig. S4A). By contrast, the endogenously expressed active Pck2 R389A potently translocated to SGs, whereas exogenously expressed inactive Pck2 barely translocated to SGs (Fig. S4B). The above data support the possibility that active Pck2 preferentially localizes to SGs. However, as these experiments were performed with exogenous expression of the active or inactive mutant Pck2, whether this reflects the physiological settings needs further study.

Temporal effect of HS on Pck2/Pmk1 MAPK signaling activation

It has been reported that HS activates various signaling pathways, including Pmk1 MAPK. To investigate the relevance of the HS-induced Pck2 subcellular distributions to PKC-mediated signaling, we assessed the downstream Pmk1 MAPK activation during HS by evaluating the phosphorylation levels of Pmk1 tagged with GST under the endogenous promoter. HS elicited acute MAPK activation within 5 min, and a gradual increase was observed upon 20 min and 60 min HS (Fig. 3A). In *pck2* deletion cells, the basal Pmk1 activity (0 min) was markedly low, and the acute MAPK activation 5 min after HS was almost abolished. Notably, the phosphorylation levels of Pmk1 in *pck2* deletion cells were almost comparable with those in WT cells upon HS for 20 min and 60 min (Fig. 3A), indicating that Pck2 is not required for Pmk1 activation at a later stage of HS responses. We then evaluated the functional involvement of Pck1 in Pmk1 activation at a later stage of HS. The results showed that Pck1 deletion increased Pmk1 phosphorylation at an early stage, and no significant change in Pmk1 activation was observed at a later stage, of HS compared with the WT cells, thus indicating that Pck1 is not involved in Pmk1 activation at the late stage of HS (Fig. 3B). Although Pck1 and Pck2 share an essential function in cell viability (Toda et al., 1993), regarding Pmk1 activation upon HS, the functional redundancy was not detected.

The HS-induced kinetics of MAPK activation and Pck2 subcellular localization suggest that Pck2 dissociates from the cell tips within 5 min upon HS, which might facilitate the acute transmission of Pck2 signaling to downstream MAPK activation. Thus, this accounts for the dependence of Pmk1 activation on Pck2 at an early stage of HS (Fig. 3A, 5 min after HS). Consistently, the kinase-negative Pck2 K712W mutation abolished MAPK activity 5 min after HS. By contrast, at a later stage of HS responses, the Pck2 mutant cells exhibited a similar MAPK activation pattern to that of the *pck2* deletion cells (Fig. 3C). Also, the cells expressing the Pck2 R389A mutant displayed higher phosphorylation levels of Pmk1 MAPK with or without HS (Fig. 3D), consistent with the constitutively active nature of Pck2 R389A kinase *in vivo*.

The *vic* phenotype (exhibiting growth in the presence of $MgCl_2$ plus the immunosuppressant FK506) is established as an indication of the downregulation of Pmk1 MAPK signaling based on the counteractive interaction between calcineurin and Pmk1 MAPK (Sio et al., 2005). Thus, this phenotype has been used as a highly sensitive biological readout for Pmk1 signaling activity *in vivo* (Ma et al., 2006; Doi et al., 2015; Sánchez-Mir et al., 2014). The Pck2 K712W mutant cells, similarly to *pmk1* deletion cells, exhibited the *vic* phenotype as indicated by their growth in medium containing 0.12 M $MgCl_2$ and FK506, wherein the WT cells failed to grow (Ma et al., 2006) (Fig. 3E). By contrast, cells harboring the constitutively active Pck2 R389A were unable to grow in the presence of 0.06 M $MgCl_2$ and FK506, whereas the WT cells grew well, showing the *vic*-negative phenotype, which is an *in vivo* indication of MAPK activation (Fig. 3E). Thus, mutations that affect Pck2 kinase activity *in vitro* influence downstream Pmk1 signaling *in vivo* by transmitting the acute responses upon HS.

Deletion of Pmk1 MAPK impairs Pck2 translocation into SGs and induces Pck2 relocalization to the cell tips

The data presented above provide evidence that Pck2 kinase activity has a stimulatory role for both Pmk1 MAPK signaling activation and Pck2 translocation into SGs upon HS. We then wanted to delineate the importance of Pck2 kinase activity or Pmk1 signaling activation in Pck2 SG translocation. To test whether Pmk1 MAPK activity plays a role in HS-induced Pck2 distribution, we expressed and imaged WT Pck2-GFP in *pmk1* deletion cells treated with HS (Fig. 4A,B). In unstressed cells, Pck2 localization in *pmk1* deletion cells was indistinguishable from that in WT cells, and Pck2 dispersal from the cell tips 5 min after HS was not substantially inhibited in *pmk1* deletion cells (Fig. 4A,B), indicating that Pmk1 deletion does not affect Pck2 dissociation from the cell tips. Strikingly, in *pmk1* deletion cells, Pck2 relocalized at the cell tips within 60 min upon HS, in contrast to the cytoplasmic (5 min) or the SG (20–60 min) Pck2 localization profile in WT cells (Fig. 4A). Conversely, Pck2 SG translocation was impaired in *pmk1* deletion cells (~50% of that in WT cells) (Fig. 4A,B). Pmk1 deletion does not affect SG assembly, as evidenced by the number of the Pabp dots (Fig. S3C) and Pck2 kinase activity (Fig. 4C), thus excluding the possibility that the

Journal of Cell Science (2021) 134, jcs250191. doi:10.1242/jcs.250191

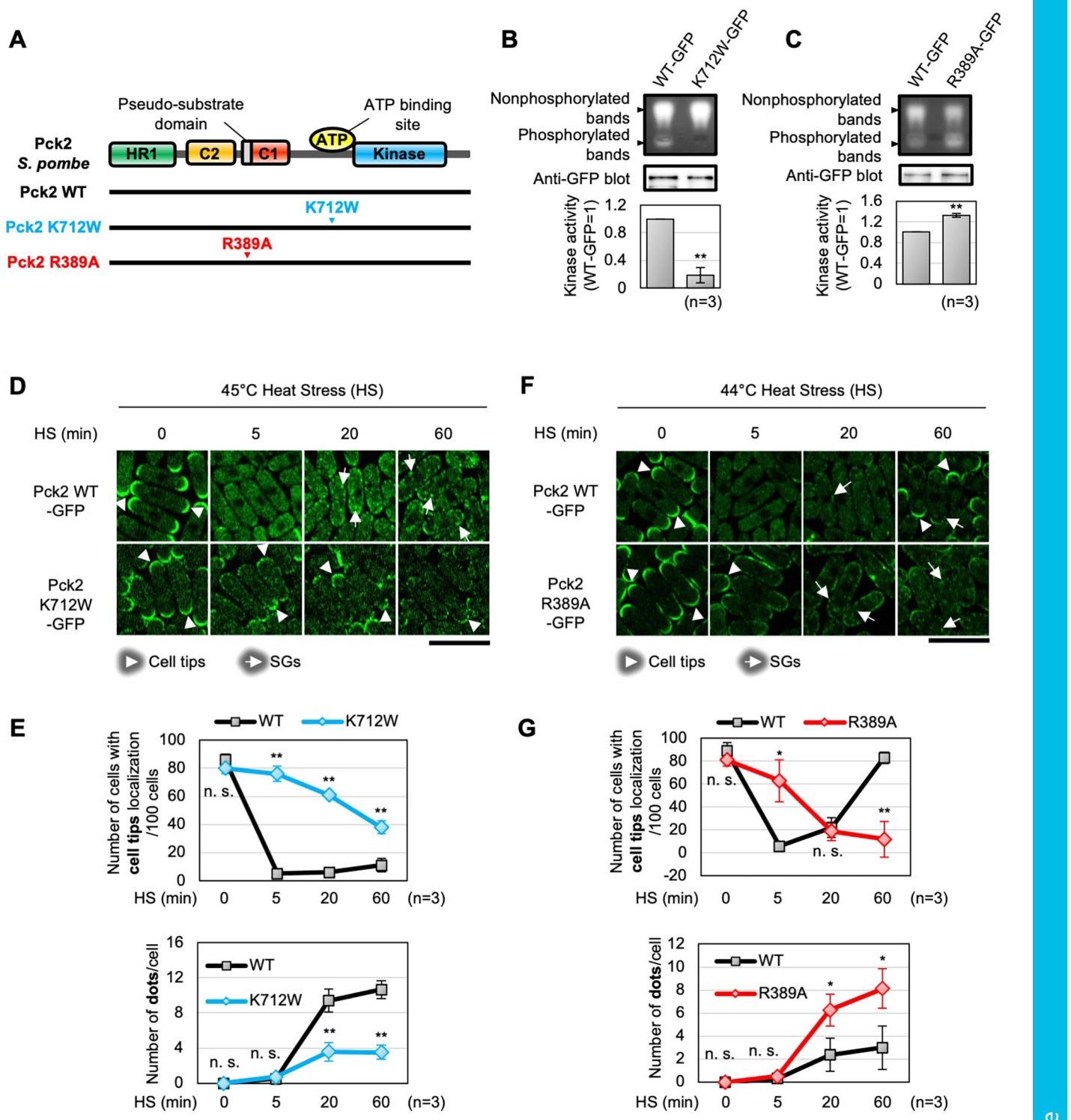

Fig. 2. See next page for legend.

observed alterations of Pck2 distribution can be induced indirectly via Pck2 or SGs. Thus, Pmk1 MAPK is required for Pck2 SG localization, but not for Pck2 dispersal from the cell tips, and Pmk1 signaling inhibition induces Pck2 relocalization to the cell tips.

Notably, the constitutively active Pck2 R389A-GFP, which exhibited a higher kinase activity and an enhanced SG localization ability in WT cells (Fig. 2C,F), exhibited markedly decreased localization at SGs in the Pmk1 deletion background compared with that of Pck2 R389A-GFP in WT cells (Fig. 4D,E, bottom). In *pmk1* deletion cells, the number of Pck2 WT dots and that of the constitutively active Pck2 R389A-GFP dots were almost the same during HS (Fig. 4B,E, bottom; Table S3). Thus, Pmk1 deletion impaired the SG localization of active Pck2 R389A. By contrast, Pck2 R389A-GFP showed increased cell tip localization in *pmk1* deletion cells compared with WT cells (Fig. 4B,E, top). These results strongly suggest that Pck2 kinase activity is required, but not

Journal of Cell Science (2021) 134, jcs250191. doi:10.1242/jcs.250191

Fig. 2. The kinase activity of Pck2 is necessary for Pck2 dispersal from the cell tips and subsequent translocation into SGs. (A) Domain structure of the PKC ortholog Pck2 (fission yeast). ATP, ATP-binding site; C1, putative diacylglycerol binding motif: C2, putative Ca^{2+}-binding motif; HR1, putative rho-binding repeat; Kinase, catalytic domain. Pck2 WT, Pck2 K712W and Pck2 R389A denote the wild-type Pck2 protein, kinase-negative Pck2 protein and constitutively active Pck2 protein, respectively. (B,C) Representative agarose gel separations of phosphorylated PepTag (top). The amounts of the corresponding GFP-fused proteins (Pck2 WT, Pck2 K712W and Pck2 R389A) that were used in the kinase reaction were shown by immunoblotting with anti-GFP antibody (middle). The levels of kinase activity were quantified and normalized as described in the Materials and Methods (bottom). Graphs show mean±s.d. (n=3). **P<0.01, significantly different from WT-GFP by Student's t-test; see Materials and Methods. (D) Kinase-dead Pck2 shows impaired translocation to SGs. Cells expressing either Pck2 WT-GFP or Pck2 K712W-GFP were observed before or after incubation at 45°C for the times indicated. Arrowheads and arrows indicate the representative cell tip localization and foci, respectively, of Pck2-GFP or Pck2 K712W-GFP. (E) The numbers of cells harboring the cell tip-localized Pck2 per 100 cells (top) or dots of Pck2 (bottom) at the indicated time points after 45°C HS are shown. Graphs show mean±s.d. (n=3). **P<0.01; n.s., not significant; significantly different from WT at each HS time point by paired Student's t-test; see Materials and Methods. (F) Constitutively active Pck2 exhibits increased translocation into SGs. The cells expressing Pck2 WT-GFP or Pck2 R389A-GFP were observed before or after incubation at 44°C for the times indicated. Arrowheads and arrows indicate the representative cell tip localization and foci, respectively, of Pck2-GFP or Pck2 R389A-GFP. (G) The numbers of cells with cell tip-localized Pck2 per 100 cells (top) or dots of Pck2 (bottom) at the indicated time points upon HS at 44°C. Graphs show mean±s.d. (n=3). *P<0.05, **P<0.01; n.s., not significant; significantly different from WT at each HS time point by paired Student's t-test; see Materials and Methods. Scale bars: 10 µm.

sufficient, for the translocation of Pck2 to SGs, and that downstream MAPK activation is crucial for determining Pck2 translocation into SGs or relocalization at the cell tips. These data indicating the existence of a delicate balance of Pck2 localization between SGs and the cell tips suggest that Pmk1 signaling inhibition may induce Pck2 cell tip relocalization by reducing SG localization.

HS at 45°C recruits Pck2 into SGs and reduces the amount and kinase activity of Pck2 in the soluble fraction

To investigate the effect of distinct HS conditions on SG formation, we treated cells with modest HS (43°C) and severe HS (45°C; referred to as HHS). Notably, HS at 43°C barely induced Pck2 dots, in contrast to HS at 45°C, which induced many Pck2 dots (~12/cell) colocalizing with Pabp (Fig. 5A–C). Importantly, HS at 43°C induced a small but significant number of Pabp dots, which appear to lack visible Pck2 dots (Fig. 5A–C). These data strongly suggested that only at 45°C (HHS), not modest HS at 43°C [low-heat stress (LHS)], led to accumulation of Pck2.

Regarding the Pck2 cell tip localization, LHS also induced Pck2 dispersal from the cell tips within 5 min, similar to HHS. However, Pck2 fully relocalized to the cell tips when cells were cultured at 43°C for 60 min, whereas Pck2 exposed to HHS remained in the SGs (Fig. 5A,B), indicating that Pck2 is more rapidly relocalized to the cell tips during recovery after HS at 43°C. Thus, SGs induced by HHS, but not by HS at 43°C, sequester Pck2, thereby impairing Pck2 localization at the cell tips, indicating the differential effect of HS (43°C and 45°C) on SG assembly and Pck2 localization.

To investigate the impact of the distinct HS conditions on the subcellular distribution and Pck2 kinase activity, we performed fractionation experiments and partitioned the cells into a 'Soluble fraction (Sup.)' and a 'Condensed fraction (Pellet)', following the scheme shown in Fig. S6A (using methods modified from Nilsson and Sunnerhagen, 2011; Wheelera et al., 2017). As shown in Fig. S6B and C, upon HHS for 20 min, Pck2, but not tubulin, partly partitioned into a Pabp-positive SG-containing fraction (Pellet) as suggested by the disappearance/decrease of Pck2/Pabp sedimentation from the pellet fraction by pre-treating the cells with CHX.

We then investigated the effect of distinct HS conditions on the subcellular distribution of Pck2 protein. The amount of Pck2-GFP immunoprecipitated from the soluble fraction by anti-GFP antibodies showed that HHS markedly reduced the abundance of Pck2 protein present in the soluble fraction (Fig. 5D). Quantification showed that, upon HHS for 60 min, the soluble fraction contained less than 5% of the Pck2 protein compared with that before HS (0 min) (Fig. 5F). By contrast, cells treated with HS at 43°C maintained more than 60% of Pck2 protein in the soluble fraction (Fig. 5F). In contrast to the soluble fraction, the pellet fraction treated with HHS accumulated a greater amount of Pck2 protein than that treated with HS (43°C) (Fig. 5F). Similarly to Pck2, HHS strongly induced Pabp partitioning from the soluble fraction into the pellet fraction, although HS (43°C) also induced significant partitioning of Pabp into the pellet fraction (Fig. 5G). These results are consistent with the observation with fluorescent microscopy that SGs induced by HHS specifically accumulated Pck2-GFP.

We then compared the *in vitro* Pck2 kinase activity immunopurified from the soluble fraction (Sup.) of the cells exposed to HS at 43°C and 45°C (Fig. 5D,E). The net Pck2 activity contained in the soluble fraction was markedly decreased when cells were treated with HHS, to ~20% of that without HS (0 min) (Fig. 5E, red). By contrast, cells treated with HS (43°C) for 60 min almost entirely retained their Pck2 kinase activity compared with that in unstressed cells (Fig. 5E, black). These results suggest that SGs induced by HHS partitioned Pck2 into a Pabp-positive pellet fraction, thereby reducing the active Pck2 protein in the soluble fraction.

Pck2 translocation to SGs upon HHS was independent of Nrd1

To investigate the impact of SGs on Pck2 localization upon HS, we expressed Pck2-GFP in several mutant backgrounds known to be defective in SG formation in *S. pombe*. These include *nrd1* deletion cells, which are reported to display impaired SG formation upon HS (Satoh et al., 2012), and the phosphorylation mutant of the translation initiation factor eIF2α (eIF2α S52A) (Nilsson and Sunnerhagen, 2011), as in mammalian cells, the key event leading to the formation of SGs is the stress-induced phosphorylation of the translation initiation factor eIF2α. In these mutant backgrounds, the endogenous Pabp was visualized, and the effects of moderate HS (43°C) and HHS (45°C) on the localization of Pabp were examined. In *nrd1* deletion cells, the number of Pabp-GFP dots was significantly decreased upon moderate HS (43°C) for 20 min and 60 min compared with that of the WT cells (Fig. 6A). However, the number of Pabp dots upon HHS (45°C) was not significantly affected by *nrd1* deletion (Fig. 6B). Moreover, Pck2-GFP dots were similarly observed in both *nrd1* deletion and WT cells during HHS (45°C) (Fig. 6C).

The number of Pabp-tdTomato dots was significantly decreased in the *eIF2α S52A* mutant cells upon moderate HS (43°C) (Fig. S5A), but not upon HHS conditions (45°C) (Fig. S5B). In addition, dynamic translocation of Pck2-GFP from the cell tips to the SGs upon HHS (45°C) was similarly observed in the *eIF2α S52A* mutant cells and WT cells (Fig. S5C). These results indicate that Pck2 translocation to SGs upon HHS was independent of Nrd1 or the phosphorylation of eIF2α, and suggest the distinct regulatory mechanism and/or structural components of SGs achieved in response to HHS.

Journal of Cell Science (2021) 134, jcs250191. doi:10.1242/jcs.250191

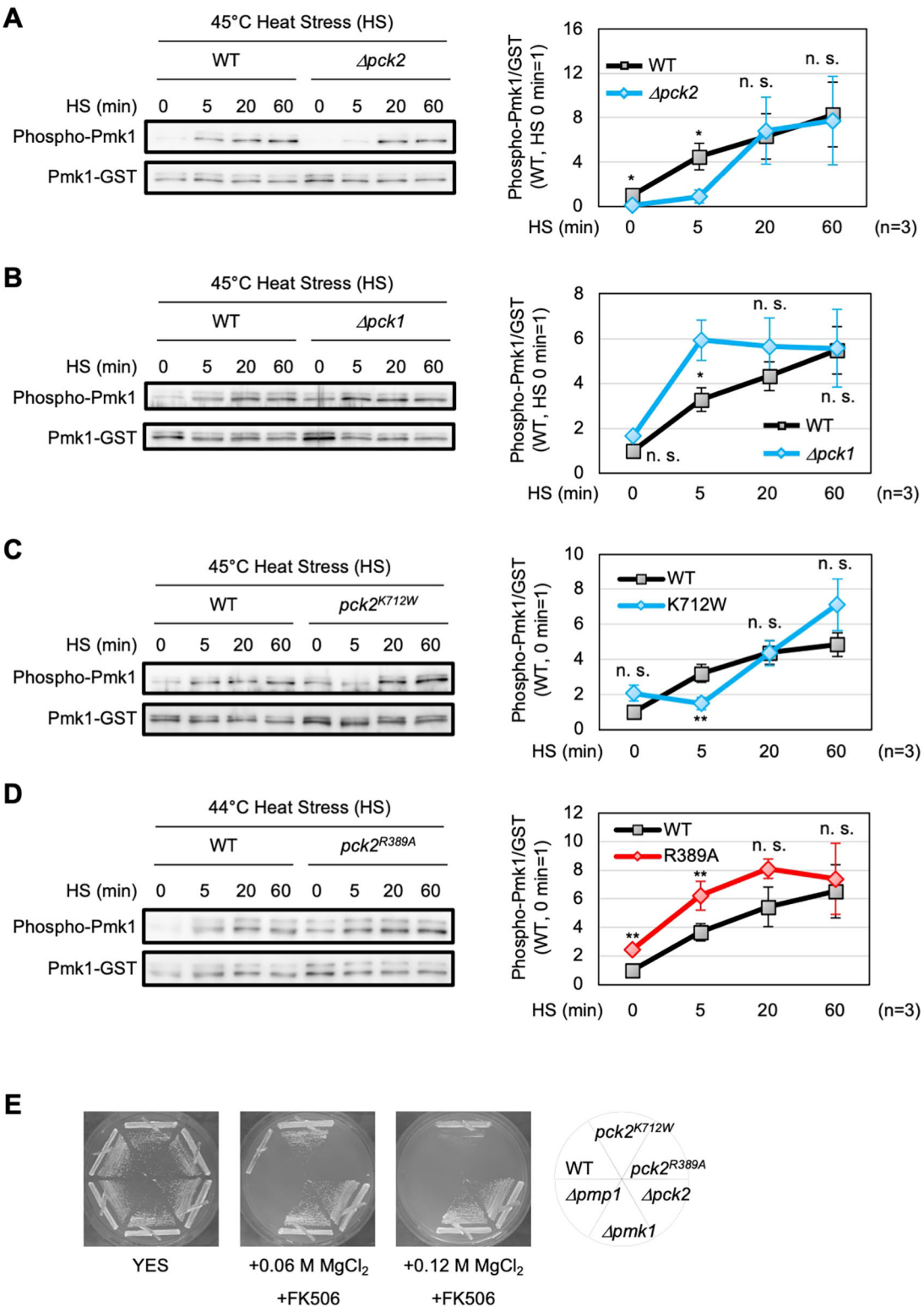

Fig. 3. Time-course analysis of the effects of Pck2 kinase activity on Pmk1 MAPK activation induced by HS. (A–D) Effects of the Pck2 deletion (A), Pck2 kinase-dead K712W mutation (B), Pck1 deletion (C) or constitutively active Pck2 R389A mutation (D) on HS-induced Pmk1 MAPK activation were evaluated by Pmk1 phosphorylation levels. Each cell was grown in EMM at 27°C for 20 h, and then incubated at 45°C or 44°C for the times indicated. Levels of Pmk1-GST purified by glutathione sepharose beads were analyzed by immunoblotting using anti-GST antibodies (Pmk1-GST) and anti-phospho-Pmk1 antibodies (phosphorylated Pmk1). Phosphorylation levels were measured as the ratio between the intensities of the phosphorylated Pmk1 and those of total Pmk1, and normalized to the levels in WT cells before HS as 1. All graphs show mean±s.d. (n=3). *P<0.05, **P<0.01; n.s., not significant; significantly different from WT at each HS time point by paired Student's t-test; see Materials and Methods. (E) The *pck2*^{K712W} mutant exhibited the *vic* (viable in the presence of Cl^-) phenotype, and the *pck2*^{R389A} mutant exhibited the *vic*-negative phenotype. WT or mutant (*pck2*^{R389A}, *pck2*^{K712W}, *Δpck2*, *Δpmk1* or *Δpmp1*) cells were grown in yeast extract with supplements (YES) or YES in the presence of 0.06 M $MgCl_2$+FK506 or 0.12 M $MgCl_2$+FK506 at 27°C for 4 days.

Journal of Cell Science (2021) 134, jcs250191. doi:10.1242/jcs.250191

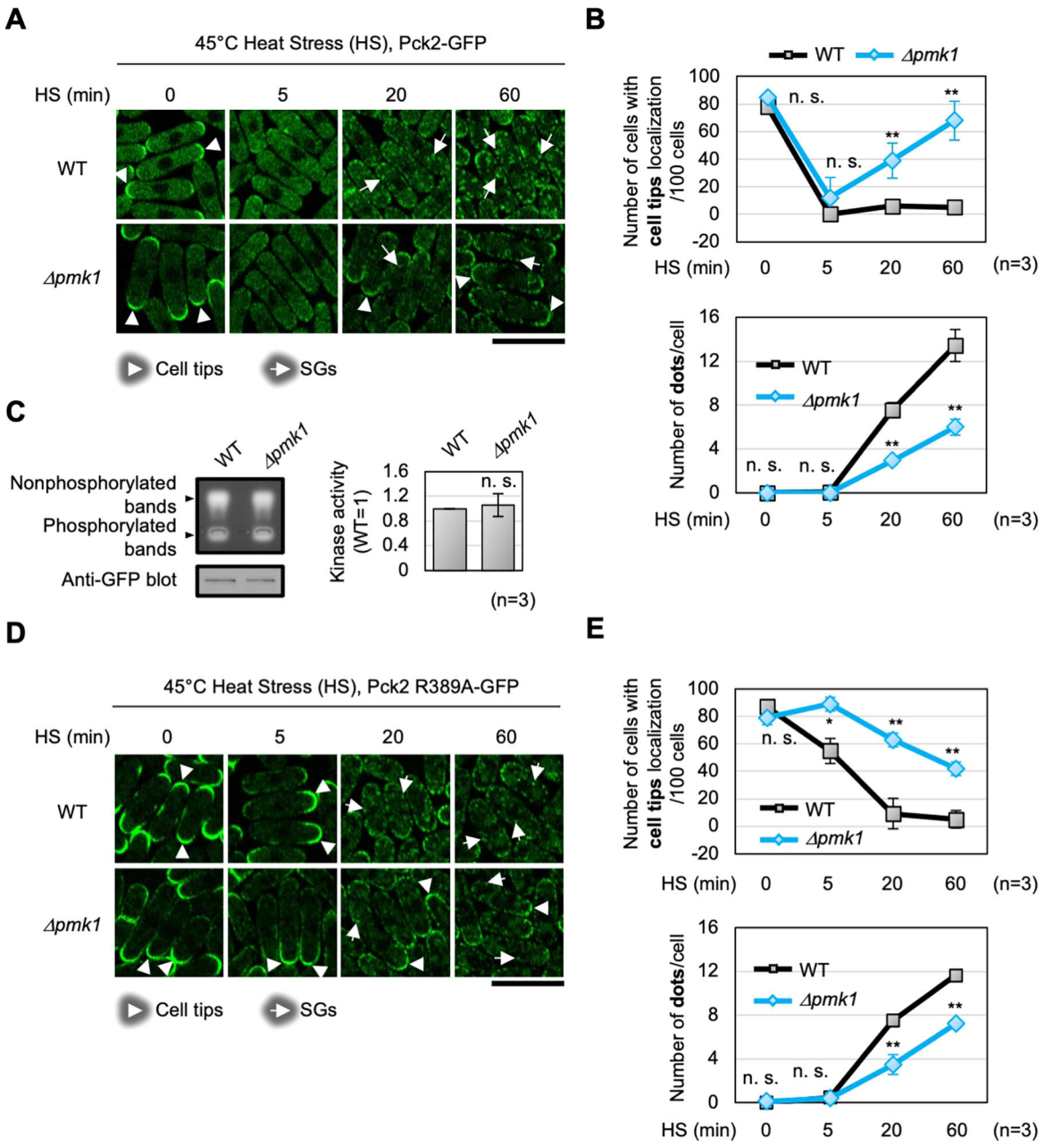

Fig. 4. Deletion of Pmk1 MAPK inhibits Pck2 SG translocation and induces Pck2 relocalization to the cell tips. (A) Localization of Pck2-GFP in WT and Pmk1-lacking cells after 45°C HS for the indicated time points. Arrowheads and arrows indicate the representative cell tip localization and foci, respectively, of Pck2-GFP. (B) Quantification of Pck2 localizations after HS at 45°C for the indicated time points. Graphs show mean±s.d. (n=3). **P<0.01; n.s., not significant; significantly different from WT at each HS time point by paired Student's t-test; see Materials and Methods. (C) Effect of Pmk1 deletion on Pck2 kinase activity. Representative agarose gel separation of phosphorylated PepTag and the corresponding amounts of GFP-fused Pck2 protein that were used in the kinase reactions are shown. The levels of kinase activity were quantified and normalized, as described in Materials and Methods. Graph shows mean±s.d. (n=3). n.s., not significant; significantly different from WT by paired Student's t-test; see Materials and Methods. (D) Localization of the constitutively active Pck2 R389A-GFP in WT and Pmk1-lacking cells after HS at 45°C for the indicated time points. Arrowheads and arrows indicate the representative cell tips localization and foci, respectively, of Pck2 R389A-GFP. (E) Quantification of Pck2 localization after HS at 45°C for the indicated time points. Graphs show mean±s.d. (n=3). *P<0.05, **P<0.01; n.s., not significant; significantly different from WT at each HS time point by paired Student's t-test; see Materials and Methods. Scale bars: 10 µm.

Pmk1 MAPK signaling is more rapidly reactivated after recovery from HS in the absence of SG formation

A recent study reported the importance of SGs on TORC1 signaling reactivation during recovery from HS (Takahara and Maeda, 2012). To investigate the significance of Pck2 sequestration into SGs, we examined whether SGs affect Pmk1 signaling during the recovery process after HS by utilizing the dynamics of SG formation and dissolution to examine whether SGs affect reactivation of Pmk1 signaling. As shown in Fig. 7A, cells were exposed to HS at 45°C (HHS) for each indicated time (0, 5, 20 and 60 min; 1st HS), then incubated at 27°C for 2 h to recover from HS (Recovery 2 h). Then, the cells were again exposed to HS for 5 min to re-stimulate Pmk1 MAPK signaling. As shown in Fig. 7A, when cells were incubated at 27°C for 2 h after the 1st HS (Recovery 2 h), Pck2 was rapidly relocalized to the cell tips, when the exposure to the 1st HS was short, and the number of Pck2 dots (upon 1st HS) was small. Pck2

Journal of Cell Science (2021) 134, jcs250191. doi:10.1242/jcs.250191

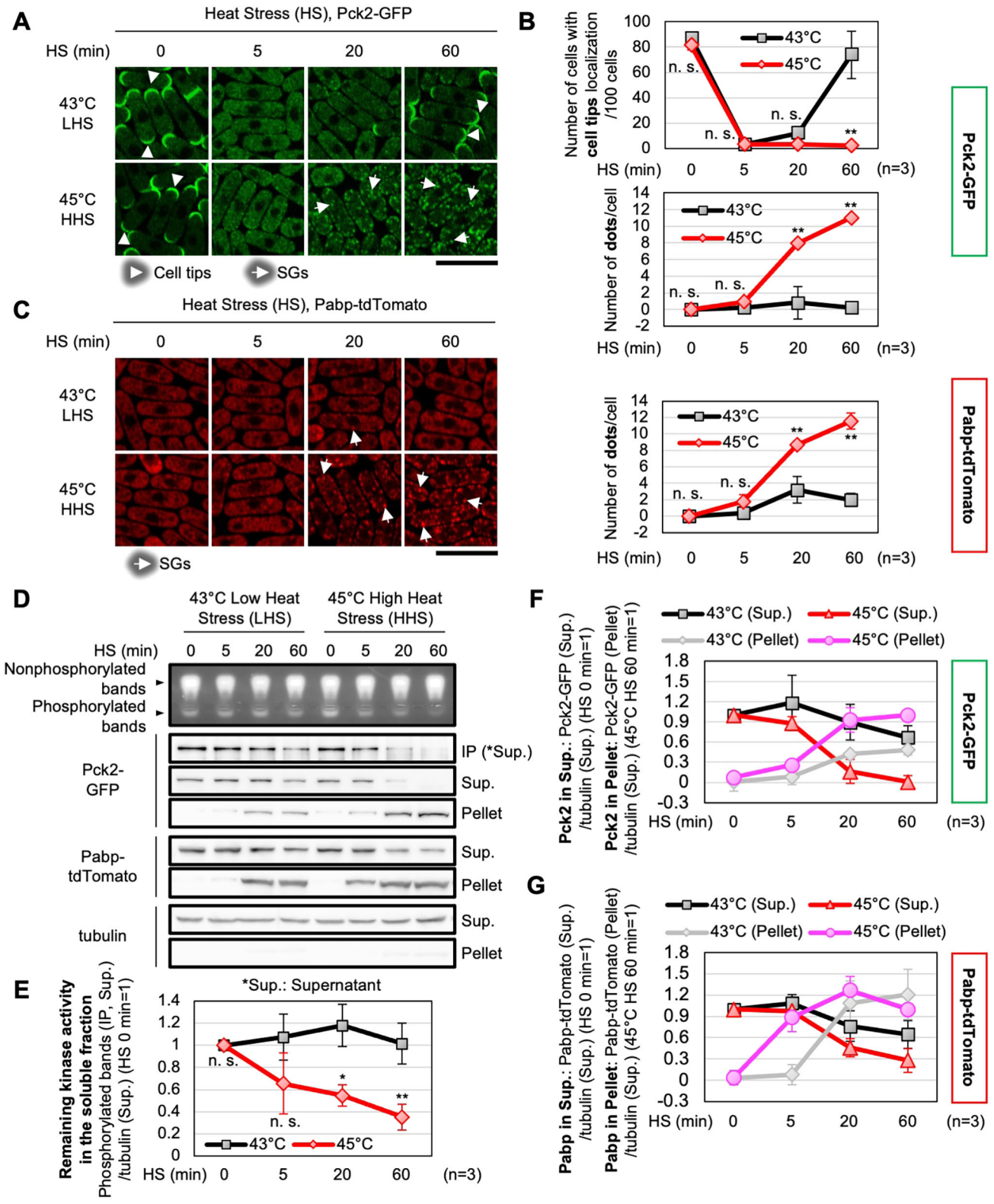

Fig. 5. See next page for legend.

did not recover its cell tip localization even after a 2 h incubation at 27°C when cells were exposed to HS for more than 20 min. A 5 min exposure to HS (1st HS) did not impair Pck2 relocalization to the cell tips after the 2 h recovery from HS, whereas a 20 min exposure impaired Pck2 cell tip relocalization, and a 60 min exposure to HS retained Pck2 in SGs (Fig. 7A).

The apparent differences in Pck2 localization after recovery from HS suggested a role for SGs in sequestration of Pck2, thereby delaying the Pck2 relocalization at cell tips. To investigate whether the subcellular localization of Pck2 before HS may impact the HS-mediated MAPK signaling activation, the MAPK phosphorylation levels among the cells before (Recovery 2 h) and after the exposure

Fig. 5. Pck2 protein and kinase activity are decreased in the soluble fraction upon high-heat stress (HHS). (A) Localization of Pck2-GFP after HS (43°C; LHS) and HHS (45°C) for the indicated times. Arrowheads and arrows indicate the representative cell tip localization and foci, respectively, of Pck2-GFP. (B) Localizations of Pck2 were quantified as analyzed in Fig. 1B. Graphs show mean±s.d. (n=3). **P<0.01; n.s., not significant; significantly different from 43°C at each HS time point by paired Student's t-test; see Materials and Methods. (C) Localizations of Pabp-tdTomato after HS (43°C; LHS) and HHS (45°C) for the indicated times. Quantification of the Pabp dots is shown on the right. Arrows indicate the foci of Pabp-tdTomato. Graphs show mean±s.d. (n=3). **P<0.01; n.s., not significant; significantly different from 43°C at each HS time point by paired Student's t-test; see Materials and Methods. (D) The kinase activity of immunoprecipitated Pck2 from the extracts of the cells exposed to the indicated HS. Immunoblots show, from top to bottom, the amount of the immunoprecipitated Pck2-GFP from soluble fractions that were used in the kinase reactions (IP), non-immunoprecipitated Pck2-GFP in the soluble (Sup.) and condensed (Pellet) fractions, Pabp-tdTomato in the soluble and condensed fractions, and tubulin in the soluble and condensed fractions. (E) Remaining kinase activity in the soluble fraction was quantified and normalized as described in the Materials and Methods. Graphs show mean±s.d. (n=3). *P<0.05, **P<0.01; n.s., not significant; significantly different from 43°C at each HS time point by paired Student's t-test; see Materials and Methods. (F,G) Protein levels of Pck2-GFP and Pabp-tdTomato in the soluble (Sup.) and condensed (Pellet) fractions that were measured and normalized as described on the left side of each graph. Graphs show mean±s.d. (n=3). Scale bars: 10 µm.

to the second HS for 5 min (2nd HS 5 min) were compared. The second HS induced Pck2 dispersal from the cell tips in cells that exhibited the cell tip Pck2 localization (Fig. 7A, 0 min and 5 min at 1st HS). This Pck2 dispersal from the cell tips resulted in acute Pmk1 activation (up to 4-fold), which is almost equivalent to that achieved by the first HS (Fig. 7B, bottom). By contrast, HS failed to activate Pmk1 MAPK when Pck2 was localized in the cytoplasm or the SGs just before the 2nd HS exposure (Fig. 6B). The above data suggest the importance of Pck2 cell tip localization in reactivation of MAPK signaling, and likewise the role of SGs in the sequestration of Pck2, thereby preventing MAPK reactivation during HS.

The same experiments were again performed in *nrd1* deletion cells wherein the SG assembly upon modest HS was defective. However, Pck2 SG translocation and Pmk1 MAPK signaling activation upon first and second HS exposure were similarly observed in *nrd1* deletion cells (Fig. 7C,D). These results further indicate the uniqueness of Pck2-positive SGs upon HHS.

DISCUSSION

In this study, we explored the role of SGs in MAPK signaling regulation and showed that SGs induced by HHS preferentially sequester Pck2/PKC in a MAPK signaling-dependent manner, thereby suggesting a role for SGs in a feedback circuit to intercept PKC/MAPK signaling activation (Fig. 8).

HS is a well-known physiological inducer of SG assembly, as well as a stimulant that activates many signaling pathways, including MAPK. However, it is poorly understood how HS-induced MAPK signaling activation is functionally connected to SG assembly. In this study, we have explored the mechanism of HS-induced Pck2 SG recruitment and its impact on MAPK signaling activation. We found that Pck2 kinase activity is required for Pck2 dispersal from the cell tips and subsequent translocation into SGs, as evidenced by the sustained cell tip localization of the kinase-negative Pck2 and the preferential recruitment of the constitutively active Pck2 mutant version into SGs upon HS. We also found that Pmk1 MAPK activation has a crucial role in Pck2 subcellular distribution, as evidenced by the decreased Pck2 translocation into SGs and increased Pck2 relocalization to the cell tips in Pmk1 deletion. Thus, Pmk1 MAPK activation promotes Pck2 SG translocation and inhibits Pck2 relocalization to the cell tips. Stimulation of the basal MAPK activity by deleting *pmp1*$^{+}$, encoding a dual-specificity MAPK phosphatase for Pmk1, enhanced Pck2 SG translocation (Fig. S7), further corroborating the importance of MAPK activation in stimulation of Pck2 SG partitioning. Importantly, the constitutively active Pck2 R389A mutant with high kinase activity failed to localize at SGs and instead exhibited a high cell tip localization profile in the Pmk1 deletion background, indicating that MAPK activity dictates whether Pck2 localizes to SGs or the cell tips. Thus, we conclude that Pck2 kinase activity is a prerequisite for Pck2 SG localization and that Pmk1 MAPK signaling activation is a critical determinant for Pck2 SG translocation.

One plausible rationale for Pmk1 activity-dependent Pck2 SG translocation is a role for SGs in a negative feedback mechanism to repress PKC/MAPK hyperactivation induced by HS. Consistently, Pmk1 deletion stimulated Pck2 relocalization to the cell tips, which is essential for stimulating Pck2-dependent MAPK activation (Kanda et al., 2016). We also presented evidence supporting the role of SGs in spatial restraint of MAPK signaling hyperactivation. Pck2 localized at the cell tips can activate Pmk1 MAPK, whereas Pck2 localized at the SGs failed to reactivate Pmk1 in response to HS (Fig. 7), showing the relevance of Pck2 distribution in HS-mediated MAPK signaling (re)activation. Thus, SGs provide a benefit as a means to avoid the detrimental effects of HS by allowing a time delay for the cell to recover the Pck2 cell tip localization by sequestering Pck2 (Fig. 8). Therefore, Pck2 recruitment into SGs resulted in repression of MAPK reactivation during recovery from HS. Various mechanisms of PKC downregulation have been reported, including protein degradation, membrane trafficking and PKC dephosphorylation, by affecting PKC protein levels and/or PKC subcellular localization from/to the plasma membrane (Newton, 2009; Madrid et al., 2017). Downregulation of PKC signaling by reducing the soluble PKC protein/activity by SGs (Fig. 7) could provide a novel way to spatiotemporally control PKC/MAPK hyperactivation, which can induce cell death under certain conditions (Gutiérrez-Venegas et al., 2009).

A similar strategy to repress MAPK signaling activation to sequester MAPK signaling regulator into SGs has been reported for RACK1, which is a signaling scaffold protein that binds to the stress-responsive MAPKKK MTK1 (Arimoto et al., 2008). SGs sequester RACK1 under HS, thereby inhibiting activation of MTK1-mediated SAPK signaling. In budding yeast, TORC1 signaling is also regulated by SGs via transient sequestration of TORC1 into SGs (Takahara and Maeda, 2012). Our study results not only present an additional example of the role of SGs as signaling hubs to sequester PKC to repress MAPK signaling, but also demonstrate the observation that SGs preferentially recruit active Pck2 in a MAPK activation-dependent manner. Based on the findings that SGs preferentially recruit Pck2 only when Pmk1 MAPK signaling is active, and that there seems to exist a threshold (45°C) for Pck2 translocation into SGs, SGs might serve as a safeguard to prevent MAPK signaling hyperactivation by sequestering active Pck2.

Our data indicate that only SGs induced by HS at 45°C (i.e. HHS) can recruit Pck2 and that deletion of *nrd1*, one of the key components of SGs, did not affect SG formation upon HHS (Figs. 5A and 6B). These data indicate the heterogeneity of SGs stimulated upon distinct stress conditions and highlight the uniqueness of the Pck2-positive SGs induced upon HHS. Currently, it remains unknown how the activation of MAPK by HHS triggers Pck2 SG translocation and the underlying molecular mechanisms that distinguish HHS from LHS. It may be intriguing to speculate that MAPK activation modulates (presumably by phosphorylation) a putative Pck2-binding partner

Journal of Cell Science (2021) 134, jcs250191. doi:10.1242/jcs.250191

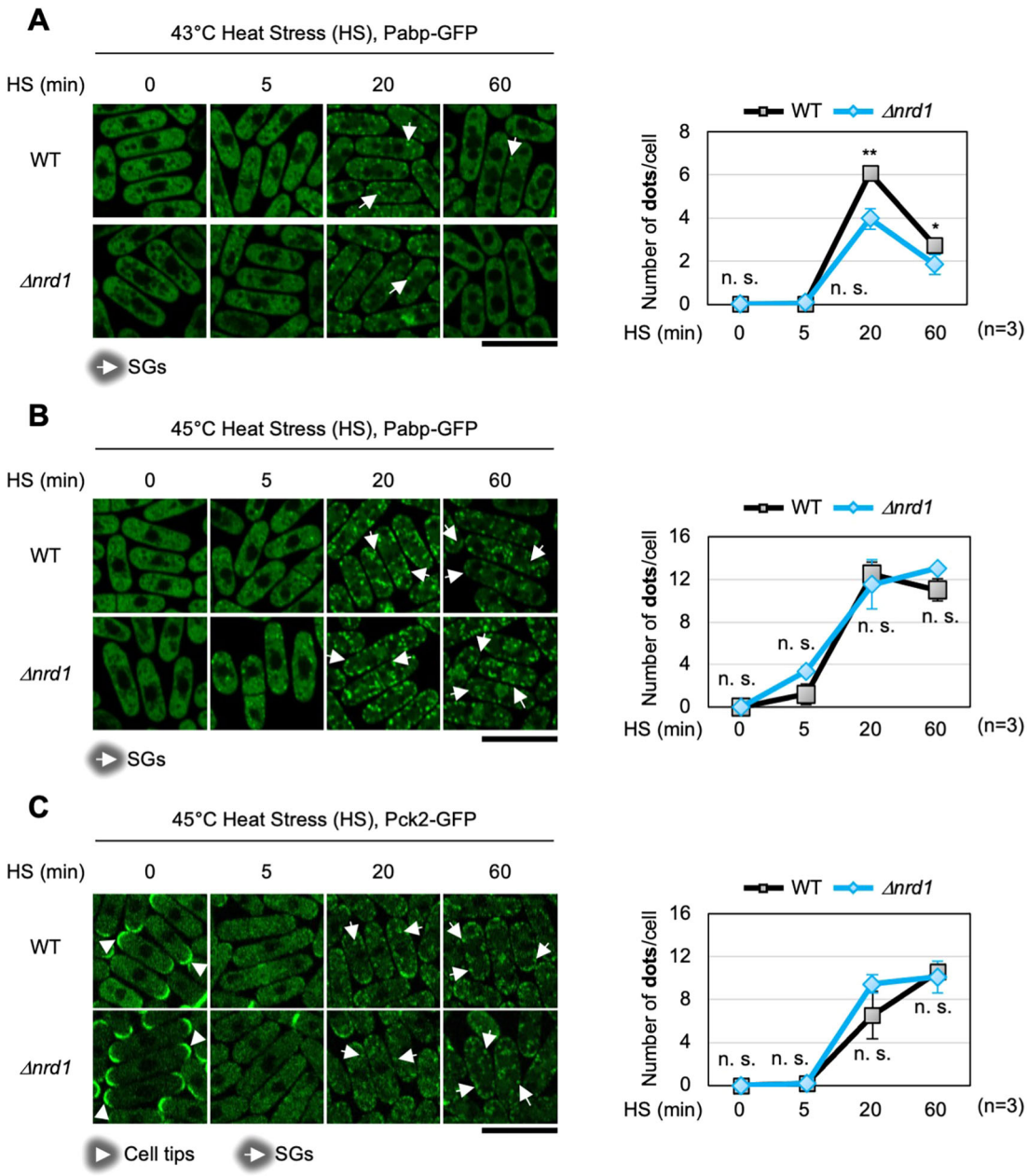

Fig. 6. Pck2 translocation to SGs upon HS was independent of Nrd1. (A,B) *nrd1* deletion cells are defective in SG assembly upon HS at 43°C, but not at 45°C. (A–C) Left: fluorescent images of the WT or *nrd1* deletion cells, expressing Pabp-GFP (A,B) or Pck2-GFP (C), exposed to HS at 43°C (A) or 45°C (B,C) for the times indicated. Right: quantification of the Pabp dots or Pck2 dots analyzed as in Fig. 1B. All graphs show mean±s.d. (n=3). *P<0.05, **P<0.01; n.s., not significant; significantly different from WT at each HS time point by paired Student's t-test; see Materials and Methods. Scale bars: 10 µm.

protein, which would facilitate Pck2 recruitment into SGs. Previous reports identified yeast Ataxin2 (Pbp1) as a negative regulator of TORC1 signaling (Yang et al., 2019). Pbp1 was shown to bind TORC1, specifically during respiratory growth, and inhibits TORC1 signaling via a low-complexity region by a phase-separation mechanism (Yang et al., 2019). Our genetic screen identified *ded1*$^{+}$ as a suppressor of MAPK signaling hyperactivation-induced cell death by Pck2 overexpression. This finding raises an intriguing possibility that Ded1, which is an SG-resident protein and an evolutionarily conserved regulator of phase separation, may suppress MAPK hyperactivation by promoting SG assembly/phase separation. Although a complete analysis and characterization of the molecular function of Ded1 in relevance to SGs and/or phase separation will form the basis of a future report, these results strongly suggest that the formation of Ded1-positive SGs appears to be relevant to repress Pck2-mediated MAPK signaling activation. Further confirmation of this view will rely on the identification of the proteins involved in SG assembly and/or Pck2 binding partners, which stimulate Pck2 SG translocation via physical interaction.

In summary, we have presented data that uncover a role for SGs as a platform to modulate the spatial distribution of Pck2, which contributes to control MAPK hyperactivation, as well as the presence of Pck2-positive granules specifically induced upon HHS. Given the importance of PKC in various physiological/pathological settings in higher organisms, our findings may shed light on the fundamental processes regulated by PKC and its control by SG assembly.

Journal of Cell Science (2021) 134, jcs250191. doi:10.1242/jcs.250191

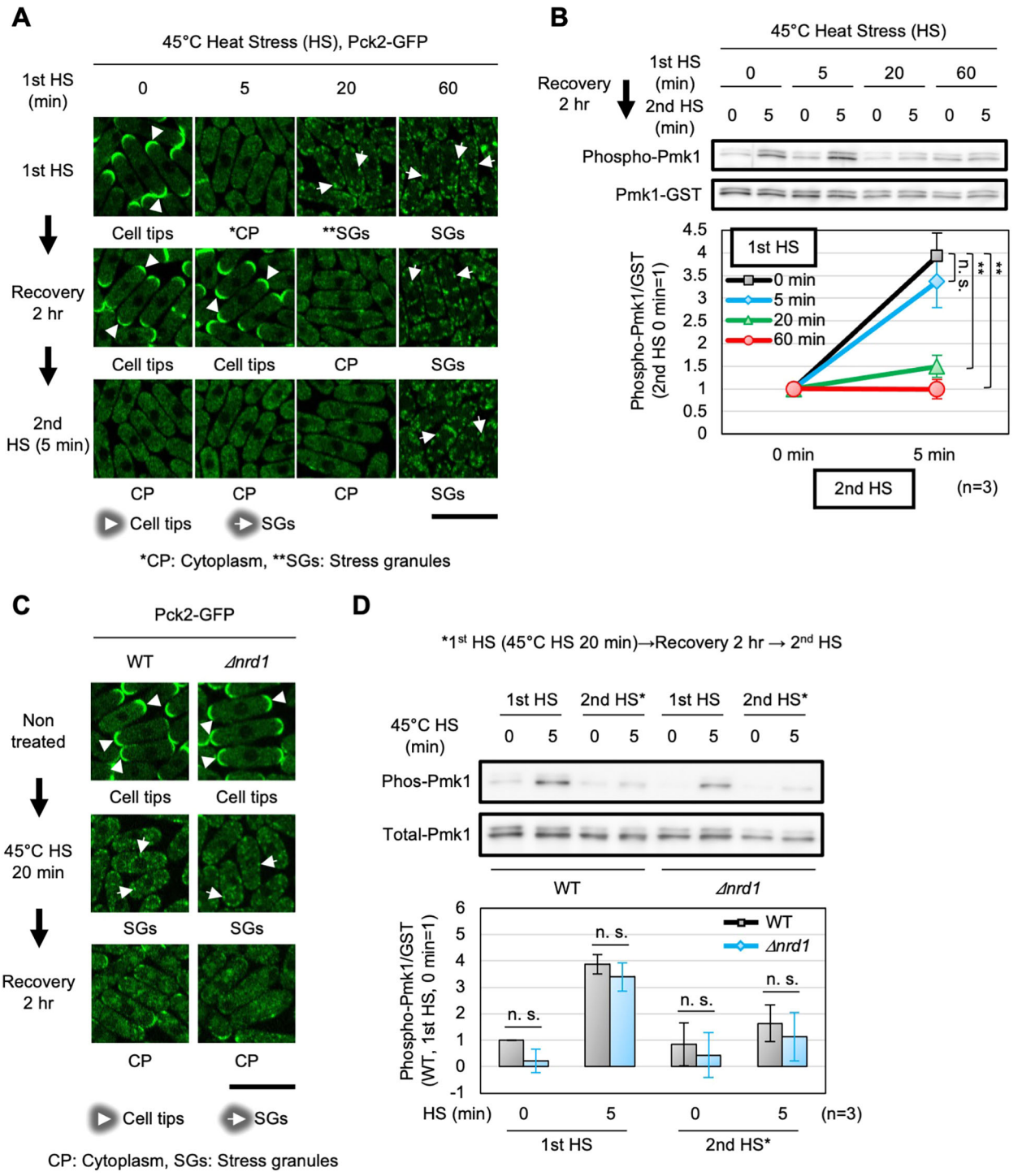

Fig. 7. Cells harboring Pck2 at the SGs cannot reactivate Pmk1 upon HS. (A) Localizations of Pck2-GFP before or after 1st HS at 45°C for the indicated time points (top), and after 2 h recovery incubation at 27°C (middle) and after 2nd HS at 45°C for 5 min (bottom). Arrowheads and arrows indicate the representative cell tip localization and foci, respectively, of Pck2-GFP. (B) Phosphorylation levels of Pmk1 before or after 2nd HS were measured and quantified as analyzed in Fig. 3. Graph shows mean±s.d. (*n*=3). ***P*<0.01; n.s., not significant; significantly different from 1st HS 0 min by Dunnett's *t*-test; see Materials and Methods. (C) Localizations of Pck2-GFP in WT and *nrd1* deletion cells before (non-treated; top) or after 1st HS at 45°C for 20 min (middle) and after 2 h recovery incubation at 27°C (bottom). (D) Phosphorylation levels of Pmk1 before or after 1st and 2nd HS in WT and *nrd1* deletion cells were measured and quantified as analyzed in Fig. 3.

Intriguingly, in mammals, PKC signaling and its deterioration are well appreciated to be closely associated with various diseases, and abnormal aggregation of PKC subtypes was reported to underlie the pathogenesis of neurodegenerative diseases such as spinocerebellar ataxia type 14 (Verbeek et al., 2008). SGs are attracting attention as RNA-centric signaling hubs to recruit many signaling molecules, and SG assembly communicates a 'state of emergency' by intercepting and sequestering components of various signaling pathways. We, therefore, assume that the MAPK-dependent PKC recruitment system involving SGs may

Journal of Cell Science (2021) 134, jcs250191. doi:10.1242/jcs.250191

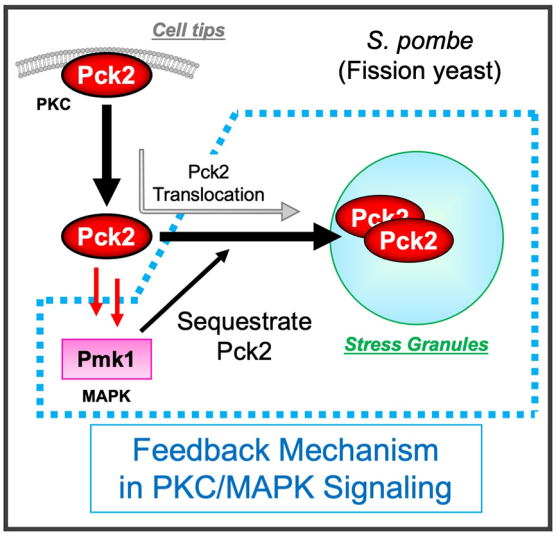

Fig. 8. Role of SGs in a feedback circuit to control MAPK signaling. HS at 45°C (HHS) induced hyperactivation of Pck2/Pmk1 MAPK signaling and Pck2 recruitment into SGs. Pck2 translocates into SGs in a kinase activity-dependent manner. The movement of Pck2 seems to represent a feedback circuit, because deletion of Pmk1 MAPK reduces Pck2 sequestration into SGs and promotes its return to the cell tips.

be a universal survival strategy that cells adapt to combat stress responses.

MATERIALS AND METHODS

Strains, media, and genetic, molecular and biological methods

Schizosaccharomyces pombe strains used in this study are listed in Table S1. The media and genetic, molecular and biological methods were as previously described (Kanda et al., 2016). Pck2 K712W and R389A were generated by inverse PCR using PrimeSTAR Max DNA Polymerase (TaKaRa). The primers used are summarized in Table S2. Proteins were C-terminally tagged with GFP, tdTomato or GST expressed from the respective endogenous loci (Bähler et al., 1998). *S. pombe* strains are described in Table S1, and we configured their authentication and tested for contamination every time.

Growth conditions and stress treatment

Unless otherwise stated, cells were cultivated at 27°C in Edinburgh minimal medium (EMM) (Sabatinos and Forsburg, 2010). Prior to stress treatment, the cells were grown to mid-log phase (optical density at a wavelength of 660 nm=0.5). HS was imposed by transferring the culture tubes to a water bath at 43°C or 45°C for the indicated time. After each stress treatment, the culture medium was chilled in ice water for 5 min. The cells were harvested by brief centrifugation at 4°C.

GST pull-down

GST pull-down was carried out as previously described (Kanda et al., 2016).

Centrifugal separation and immunoprecipitation

The scheme for centrifugal separation is shown in Fig. S6A. Protein lysates were prepared in lysis buffer [1% Triton X-100, 30 mM Tris-HCl (pH 8.0), 2 mM EDTA]. Lysates were centrifuged at 800 ***g*** for 3 min, and then the supernatants were collected. Subsequently, the supernatants were centrifuged at 815 ***g*** or 3300 ***g*** for 15 min, and then the supernatants were collected (soluble fraction). The pellets after the second centrifugation were washed in lysis buffer and centrifuged at 815 ***g*** or 3300 ***g*** for 15 min again. After the removal of the supernatants, the pellets were collected (condensed fraction). GFP-tagged proteins were immunoprecipitated (IP) using anti-GFP antibody (Ma et al., 2006) with Pierce TM Protein A/G Magnetic Beads (Thermo Fisher Scientific, 88803).

Protein detection

Antibodies used are listed in Table S2. Membranes were developed with Chemi-Lumi One Super (Nacalai Tesque, Japan). Protein levels were quantified using relative intensities of all bands that were quantified using MULTI GAUGE Ver. 3.2 software (Fujifilm, Japan).

PKC activity assay

PKC activity was measured by the PepTag® assay (Promega, Japan) as previously reported (Sukumaran and Prasadarao, 2002; Shao and Bayraktutan, 2013). *In vitro* kinase reaction was performed at 30°C for 30 min in a mixture of purified PKC (primarily of α, β and γ isoforms with lesser amounts of δ and ζ isoforms; Walton et al., 1987), GST- or GFP-tagged Pck2 mutants [purified by IP; described in the 'Centrifugal separation and immunoprecipitation (IP)' section] and 25 µl of the PepTag® solution containing 5 µl 5×PKC reaction buffer, 1 µl P-L-S-R-T-L-S-V-A-A-K peptide, 1 µl peptide protection solution and 18 µl ultra-pure water. The reaction was terminated at 95°C for 10 min. Each sample was separated by electrophoresis using a 1.0% agarose gel at 100 V for 20 min. The phosphorylated peptide was quantified using ImageJ software (http://rsb.info.nih.gov/ij/). Protein kinase activity was analyzed for the level of total Pck2 by western blotting and the phosphorylated peptide (Figs. 2B,C and 4C). Given the varying nature of the Pck2 protein levels in the soluble fraction upon heat stress, the net kinase activity of Pck2 from the soluble fraction was analyzed by western blotting for the level of tubulin from the soluble fraction as a loading control and the phosphorylated peptide (Fig. 7D).

Microscopy and miscellaneous methods

Microscopy and miscellaneous methods were carried out as previously described (Kanda et al., 2016).

Image quantification

The quantification of cell tip localization was performed for at least two individual datasets, which analyzed up to 100 cells. Quantification of stress granules foci was performed for at least two individual datasets, which summed up to 50 counted cells.

Statistical analysis

All results are expressed as mean±s.d. of several independent experiments. Data were analyzed using a one-way ANOVA, followed by Student's *t*-test (Figs. 1F, 2B,C,E,G, 3A–D, 4B,C,E, 5B,C,E, 6A,B,C, 7D; Figs. S2B, S3A–C, S5A–C, S7B) or one-way ANOVA, followed by a post hoc test using Dunnett's multiple comparison (Fig. 6B). *P*-values less than 0.05 were regarded as significant.

Acknowledgements

We thank Dr T. Toda and the Yeast Resource Center (YGRC/NBRP; http://yeast.lab.nig.ac.jp/nig) for providing strains and plasmids; and Professor William Figoni for critical reading of the manuscript. We are grateful to the members of the Laboratory of Molecular Pharmacogenomics for their support.

Competing interests

The authors declare no competing or financial interests.

Author contributions

Conceptualization: Y.K., R. Satoh, T. Takasaki, K.H., T.F., R. Sugiura; Methodology: Y.K., R. Satoh, T. Takasaki, K.H., T.F., R. Sugiura; Validation: Y.K., R. Satoh, T. Takasaki, K.H., R. Sugiura; Formal analysis: Y.K., R. Satoh, T. Takasaki, N.T., K.T., C.A.T., T. Tanaka, S.K., K.H., R. Sugiura; Investigation: Y.K., N.T., K.T., C.A.T., T. Tanaka, S.K.; Resources: R. Sugiura; Data curation: Y.K.; Writing - original draft: Y.K., R. Sugiura; Writing - review & editing: Y.K., R. Satoh, T. Takasaki, K.H., T.F., R. Sugiura; Visualization: Y.K., R. Sugiura; Supervision: R. Sugiura; Project administration: R. Sugiura; Funding acquisition: R. Sugiura.

Funding

This study was supported by the Ministry of Education, Culture, Sports, Science and Technology (MEXT)-Supported Program for the Strategic Research Foundation at Private Universities, 2014–2018 [JPS1411037 (R. Sugiura)], a Grant-in-Aid for scientific research from the Japan Society for the Promotion of Science (JSPS) KAKENHI [JP19H03376 (R. Sugiura)], a JSPS Fellowship [JP20J15403 (Y.K.)] and a grant by the Antiaging Project for Private Universities (R. Sugiura).

Supplementary information

Supplementary information available online at
https://jcs.biologists.org/lookup/doi/10.1242/jcs.250191.supplemental

Peer review history

The peer review history is available online at
https://jcs.biologists.org/lookup/doi/10.1242/jcs.250191.reviewer-comments.pdf

References

Anderson, P. and Kedersha, N. (2006). RNA granules. *J. Cell Biol.* **172**, 803-808. doi:10.1083/jcb.200512082

Anderson, P. and Kedersha, N. (2009). RNA granules: post-transcriptional and epigenetic modulators of gene expression. *Nat. Rev. Mol. Cell Biol.* **10**, 430-436. doi:10.1038/nrm2694

Arellano, M., Valdivieso, M. H., Calonge, T. M., Coll, P. M., Duran, A. and Perez, P. (1999). *Schizosaccharomyces pombe* protein kinase C homologues, pck1p and pck2p, are targets of rho1p and rho2p and differentially regulate cell integrity. *J. Cell Sci.* **112**, 3569-3578.

Arimoto, K., Fukuda, H., Imajoh-Ohmi, S., Saito, H. and Takekawa, M. (2008). Formation of stress granules inhibits apoptosis by suppressing stress-responsive MAPK pathways. *Nat. Cell Biol.* **10**, 1324-1332. doi:10.1038/ncb1791

Bähler, J., Wu, J.-Q., Longtine, M. S., Shah, N. G., McKenzie, A., III, Steever, A. B., Wach, A., Philippsen, P. and Pringle, J. R. (1998). Heterologous modules for efficient and versatile PCR-based gene targeting in *Schizosaccharomyces pombe*. *Yeast* **14**, 943-951. doi:10.1002/(SICI)1097-0061(199807)14:10<943::AID-YEA292>3.0.CO;2-Y

Brambilla, M., Martani, F. and Branduardi, P. (2017). The recruitment of the *Saccharomyces cerevisiae* poly(A)-binding protein into stress granules: new insights into the contribution of the different protein domains. *FEMS Yeast Res.* **17**, fox059. doi:10.1093/femsyr/fox059

Callender, J. A. and Newton, A. C. (2017). Conventional protein kinase C in the brain: 40 years later. *Neuronal. Signal.* **1**, NS20160005. doi:10.1042/NS20160005

Doi, A., Kita, A., Kanda, Y., Uno, T., Asami, K., Satoh, R., Nakano, K. and Sugiura, R. (2015). Geranylgeranyltransferase Cwg2-Rho4/Rho5 module is implicated in the Pmk1 MAP Kinase-mediated cell wall integrity pathway in fission yeast. *Genes Cells* **20**, 310-323. doi:10.1111/gtc.12222

Fuchs, B. B. and Mylonakis, E. (2009). Our paths might cross: the role of the fungal cell wall integrity pathway in stress response and cross talk with other stress response pathways. *Eukaryot. Cell* **8**, 1616-1625. doi:10.1128/EC.00193-09

Gould, C. M. and Newton, A. C. (2008). The life and death of protein kinase C. *Curr. Drug Targets* **9**, 614-625. doi:10.2174/138945008785132411

Grallert, B., Kearsey, S. E., Lenhard, M., Carlson, C. R., Nurse, P., Boye, E. and Labib, K. (2000). A fission yeast general translation factor reveals links between protein synthesis and cell cycle controls. *J. Cell Sci.* **113**, 1447-1458.

Guil, S., Long, J. C. and Cáceres, J. F. (2006). hnRNP A1 relocalization to the stress granules reflects a role in the stress response. *Mol. Cell Biol.* **26**, 5744-5758. doi:10.1128/MCB.00224-06

Gutiérrez-Venegas, G., Arreguín-Cano, J. A., Arroyo-Cruz, R., Villeda-Navarro, M. and Méndez-Mejía, J. A. (2009). Activation of ERK1/2 by protein kinase C-α in response to hydrogen peroxide-induced cell death in human gingival fibroblasts. *Toxicol. In Vitro.* **24**, 319-326. doi:10.1016/j.tiv.2009.08.007

Higa, M., Kita, A., Hagihara, K., Kitai, Y., Doi, A., Nagasoko, R., Satoh, R. and Sugiura, R. (2015). Spatial control of calcineurin in response to heat shock in fission yeast. *Genes Cells* **20**, 95-107. doi:10.1111/gtc.12203

Hilliker, A., Gao, Z., Jankowsky, E. and Parker, R. (2011). The DEAD-box protein ded1 modulates translation by the formation and resolution of an eIF4F-mRNA complex. *Mol. Cell* **43**, 962-972. doi:10.1016/j.molcel.2011.08.008

Hoyer, K. K., Herling, M., Bagrintseva, K., Dawson, D. W., French, S. W., Renard, M., Weinger, J. G., Jones, D. and Teitell, M. A. (2005). T cell leukemia-1 modulates TCR signal strength and IFN-γ levels through phosphatidylinositol 3-kinase and protein kinase C pathway activation. *J. Immunol.* **175**, 864-873. doi:10.4049/jimmunol.175.2.864

Isakov, N. (2018). Protein kinase C (PKC) isoforms in cancer, tumor promotion and tumor suppression, Semin. *Cancer Biol.* **48**, 36-52. doi:10.1016/j.semcancer.2017.04.012

Kanda, Y., Satoh, R., Matsumoto, S., Ikeda, C., Inutsuka, N., Hagihara, K., Matzno, S., Tsujimoto, S., Kita, A. and Sugiura, R. (2016). Skb5, an SH3 adaptor protein, regulates Pmk1 MAPK signaling by controlling the intracellular localization of the MAPKKK Mkh1. *J. Cell Sci.* **129**, 3189-3202. doi:10.1242/jcs.188854

Kedersha, N. and Anderson, P. (2007). Mammalian stress granules and processing bodies. *Methods Enzymol.* **431**, 61-81. doi:10.1016/S0076-6879(07)31005-7

Kedersha, N., Cho, M. R., Li, W., Yacono, P. W., Chen, S., Gilks, N., Golan, D. E. and Anderson, P. (2000). Dynamic shuttling of TIA-1 accompanies the recruitment of mRNA to mammalian stress granules. *J. Cell Biol.* **151**, 1257-1268. doi:10.1083/jcb.151.6.1257

Kobayashi, T., Winslow, S., Sunesson, L., Hellman, U. and Larsson, C. (2012). PKCα binds G3BP2 and regulates stress granule formation following cellular stress. *PLoS ONE* **7**, e35820. doi:10.1371/journal.pone.0035820

Li, Z., Wang, N., Fang, J., Huang, J., Tian, F., Li, C. and Xie, F. (2012). Role of PKC-ERK signaling in tamoxifen-induced apoptosis and tamoxifen resistance in human breast cancer cells. *Oncol. Rep.* **27**, 1879-1886.

Lucke-Wold, B. P., Turner, R. C., Logsdon, A. F., Simpkins, J. W., Alkon, D. L., Smith, K. E., Chen, Y.-W., Tan, Z., Huber, J. D. and Rosen, C. L. (2015). Common mechanisms of Alzheimer's disease and ischemic stroke: the role of protein kinase C in the progression of age-related neurodegeneration. *J. Alzheimers Dis.* **43**, 711-724. doi:10.3233/JAD-141422

Ma, Y., Kuno, T., Kita, A., Asayama, Y. and Sugiura, R. (2006). Rho2 is a target of the farnesyltransferase Cpp1 and acts upstream of Pmk1 mitogen-activated protein kinase signaling in fission yeast. *Mol. Biol. Cell* **17**, 5028-5037. doi:10.1091/mbc.e06-08-0688

Madrid, M., Jiménez, R., Sánchez-Mir, L., Soto, T., Franco, A., Vicente-Soler, J., Gacto, M., Pérez, P. and Cansado, J. (2015). Multiple layers of regulation influence cell integrity control by the PKC ortholog Pck2 in fission yeast. *J. Cell Sci.* **128**, 266-280. doi:10.1242/jcs.158295

Madrid, M., Vázquez-Marín, B., Soto, T., Franco, A., Gómez-Gil, E., Vicente-Soler, J., Gacto, M., Pérez, P. and Cansado, J. (2017). Differential functional regulation of protein kinase C (PKC) orthologs in fission yeast. *J. Biol. Chem.* **292**, 11374-11387. doi:10.1074/jbc.M117.786087

Mazroui, R., Huot, M. E., Tremblay, S., Filion, C., Labelle, Y. and Khandjian, E. W. (2002). Trapping of messenger RNA by Fragile X Mental Retardation protein into cytoplasmic granules induces translation repression. *Hum. Mol. Gen.* **15**, 3007-3017. doi:10.1093/hmg/11.24.3007

Mollet, S., Cougot, N., Wilczynska, A., Dautry, F., Kress, M., Bertrand, E. and Weil, D. (2008). Translationally repressed mRNA transiently cycles through stress granules during stress. *Mol. Biol. Cell* **19**, 4469-4479. doi:10.1091/mbc.e08-05-0499

Mukai, H. (2003). The Structure and Function of PKN, a Protein Kinase Having a Catalytic Domain Homologous to That of PKC. *J. Biochem.* **133**, 17-27. doi:10.1093/jb/mvg019

Newton, A. C. (2009). Lipid activation of protein kinases. *J. Lipid Res.* **50**, 266-271. doi:10.1194/jlr.R800064-JLR200

Newton, A. C. (2010). Protein kinase C: poised to signal. *Am. J. Physiol. Endocrinol. Metab.* **298**, E395-E402. doi:10.1152/ajpendo.00477.2009

Newton, A. C. and Jhonson, J. E. (1998). Protein kinase C: a paradigm for regulation of protein function by two membrane-targeting modules. *Biochim. Biophys. Acta* **1376**, 155-172. doi:10.1016/S0304-4157(98)00003-3

Nilsson, D. and Sunnerhagen, P. (2011). Cellular stress induces cytoplasmic RNA granules in fission yeast. *RNA* **17**, 120-133. doi:10.1261/rna.2268111

Panas, M. D., Ivanov, P. and Anderson, P. (2016). Mechanistic insights into mammalian stress granule dynamics. *J. Cell Biol.* **215**, 313-323. doi:10.1083/jcb.201609081

Pintus, G., Tadolini, B., Posadino, A. M., Sanna, B., Debidda, M., Carru, C., Deiana, L. and Ventura, C. (2003). PKC/Raf/MEK/ERK signaling pathway modulates native-LDLinduced E2F-1 gene expression and endothelial cell proliferation. *Cardiovasc. Res.* **59**, 934-944. doi:10.1016/S0008-6363(03)00526-1

Sabatinos, S. A. and Forsburg, S. L. (2010). Molecular genetics of *Schizosaccharomyces pombe*. *Methods Enzymol.* **470**, 759-795. doi:10.1016/S0076-6879(10)70032-X

Sánchez-Mir, L., Soto, T., Franco, A., Madrid, M., Viana, R. A., Vicente, L., Gacto, M., Pérez, P. and Cansado, J. (2014). Rho1 GTPase and PKC ortholog Pck1 are upstream activators of the cell integrity MAPK pathway in fission yeast. *PLoS ONE* **9**, e88020. doi:10.1371/journal.pone.0088020

Satoh, R., Tanaka, A., Kita, A., Morita, T., Matsumura, Y., Umeda, N., Takada, M., Hayashi, S., Tani, T., Shinmyozu, K. et al. (2012). Role of the RNA-binding protein Nrd1 in stress granule formation and its implication in the stress response in fission yeast. *PLoS ONE* **7**, e29683. doi:10.1371/journal.pone.0029683

Sayers, L. G., Katayama, S., Nakano, K., Mellor, H., Mabuchi, I., Toda, T. and Parker, P. J. (2000). Rho-dependence of *Schizosaccharomyces pombe* Pck2. *Genes Cells* **5**, 17-27. doi:10.1046/j.1365-2443.2000.00301.x

Shao, B. and Bayraktutan, U. (2013). Hyperglycaemia promotes cerebral barrier dysfunction through activation of protein kinase C-β. *Diabetes. Obes. Metab.* **15**, 993-999. doi:10.1111/dom.12120

Sio, S. O., Suehiro, T., Sugiura, R., Takeuchi, M., Mukai, H. and Kuno, T. (2005). The role of the regulatory subunit of fission yeast calcineurin for in vivo activity and its relevance to FK506 sensitivity. *J. Biol. Chem.* **280**, 12231-12238. doi:10.1074/jbc.M414234200

Sugiura, R., Toda, T., Shuntoh, H., Yanagida, M. and Kuno, T. (1998). *pmp1*$^{+}$, a suppressor of calcineurin deficiency, encodes a novel MAP kinase phosphatase in fission yeast. *EMBO J.* **17**, 140-148. doi:10.1093/emboj/17.1.140

Sukumaran, S. K. and Prasadarao, N. V. (2002). Regulation of protein kinase C in Escherichia coli K1 invasion of human brain microvascular endothelial cells. *J. Biol. Chem.* **277**, 12253-12262. doi:10.1074/jbc.M110740200

Takada, H., Nishimura, M., Asayama, Y., Mannse, Y., Ishiwata, S., Kita, A., Doi, A., Nishida, A., Kai, N., Moriuchi, S. et al. (2007). Atf1 is a target of the mitogen-

activated protein kinase Pmk1 and regulates cell integrity in fission yeast. *Mol. Biol. Cell* **18**, 4794-4802. doi:10.1091/mbc.e07-03-0282

Takahara, T. and Maeda, T. (2012). Transient sequestration of TORC1 into stress granules during heat stress. *Mol. Cell* **47**, 242-252. doi:10.1016/j.molcel.2012.05.019

Thedieck, K., Holzwarth, B., Prentzell, M. T., Boehlke, C., Kläsener, K., Ruf, S., Sonntag, A. G., Maerz, L., Grellscheid, S.-N., Kremmer, E. et al. (2013). Inhibition of mTORC1 by astrin and stress granules prevents apoptosis in cancer cells. *Cell* **154**, 859-874. doi:10.1016/j.cell.2013.07.031

Toda, T., Shimanuki, M. and Yanagida, M. (1993). Two novel protein kinase C-related genes of fission yeast are essential for cell viability and implicated in cell shape control. *EMBO J.* **12**, 1987-1995. doi:10.1002/j.1460-2075.1993.tb05848.x

Toda, T., Dhut, S., Superti-Furga, G., Gotoh, Y., Nishida, E., Sugiura, R. and Kuno, T. (1996). The fission yeast *pmk1*$^{+}$ gene encodes a novel mitogen-activated protein kinase homolog which regulates cell integrity and functions coordinately with the protein kinase C pathway. *Mol. Cell. Biol.* **16**, 6752-6764. doi:10.1128/MCB.16.12.6752

Verbeek, D. S., Goedhart, J., Bruinsma, L., Sinke, R. J. and Reits, E. A. (2008). PKC gamma mutations in spinocerebellar ataxia type 14 affect C1 domain accessibility and kinase activity leading to aberrant MAPK signaling. *J. Cell Sci.* **121**, 2339-2349. doi:10.1242/jcs.027698

Walton, G. M., Bertics, P. J., Hudson, L. G., Vedvick, T. S. and Gill, G. N. (1987). A three-step purification procedure for protein kinase C: characterization of the purified enzyme. *Anal. Biochem.* **161**, 425-437. doi:10.1016/0003-2697(87)90471-4

Watanabe, M., Chen, C. and Levin, D. E. (1994). *Saccharomyces cerevisiae* PKC1 Encodes a Protein Kinase C (PKC) homolog with a substrate specificity similar to that of mammalian PKC. *J. Biol. Chem.* **269**, 16829-16836.

Wheelera, J. R., Jain, S., Khonga, A. and Parker, R. (2017). Isolation of yeast and mammalian stress granule cores. *Methods* **126**, 12-17. doi:10.1016/j.ymeth.2017.04.020

Wippich, F., Bodenmiller, B., Trajkovska, M. G., Wanka, S., Aebersold, R. and Pelkmans, L. (2013). Dual specificity kinase DYRK3 couples stress granule condensation/dissolution to mTORC1 signaling. *Cell* **152**, 791-805. doi:10.1016/j.cell.2013.01.033

Yang, Y.-S., Kato, M., Wu, X., Litsios, A., Sutter, B. M., Wang, Y., Hsu, C.-H., Wood, N. E., Lemoff, A., Mirzaei, H. et al. (2019). Yeast Ataxin-2 forms an intracellular condensate required for the inhibition of TORC1 signaling during respiratory growth. *Cell* **177**, 697-710.e17. doi:10.1016/j.cell.2019.02.043

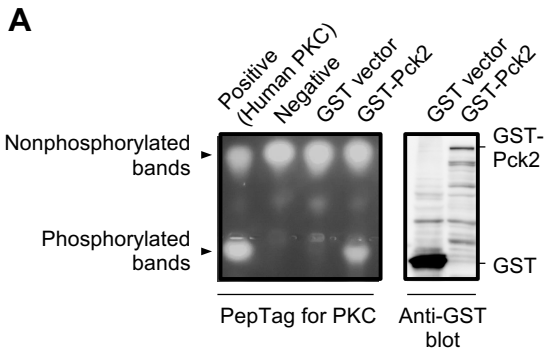

Kanda et al. Supplementary Figure S1

Figure S1. PepTag analysis of the fission yeast Pck2

(A) In vitro kinase activity of the fission yeast Pck2. Left panel: Representative agarose gel separation of phosphorylated PepTag showing fluorescent phosphorylated Peptag. Right panel: Immunoblotting analysis showing the expression of purified GST and GST-fused Pck2 proteins used for the experiments in Figure S1A. GST pull-downs carried out with GST or GST-Pck2; Cells transformed with plasmids harboring GST alone (vector) or GST-Pck2, were collected and the lysates were incubated with glutathione beads. Proteins purified by glutathione sepharose were analyzed by SDS-PAGE and immunoblotted using anti-GST antibodies. Mammalian PKC and water were added as a positive and negative control, respectively.

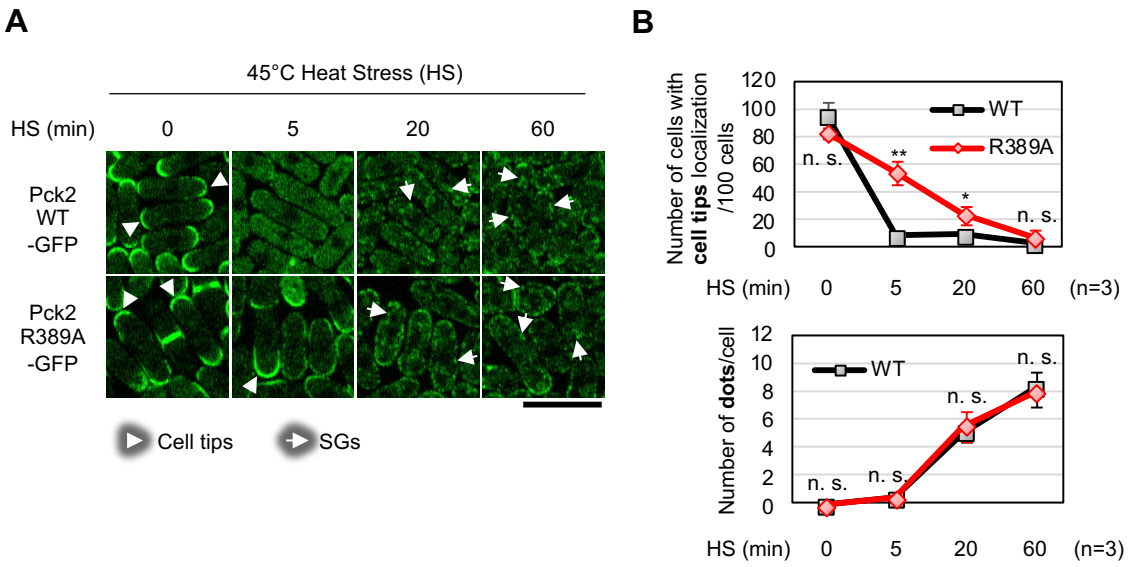

Kanda et al. Supplementary Figure S2

Figure S2. HS at 45°C does not discriminate between Pck2 WT-GFP and Pck2 R389A-GFP in terms of their subcellular distribution at the SGs

(A) Fluorescent images of cells expressing the Pck2 WT-GFP or the Pck2 R389A-GFP mutant protein from the endogenous promoter with HS (45°C) for the times indicated. Arrowheads and arrows indicate the representative cell tips localization and foci of Pck2-GFP or Pck2 R389A-GFP, respectively. Scale bars 10 µm. (B) upper panel: Quantification of the cells in Figure S2A showing the Pck2 cell-tip localization analyzed, as indicated in Figure 1B. lower panel: Quantification of Pck2 dots in cells shown in Figure S2A analyzed, as indicated in Figure 1B. Graphs show mean ± s.d. (n=3). *P<0.05, **P<0.01 n.s.: not significant; significantly different from 43°C in each HS time point by Student's t-test; see Materials and Methods.

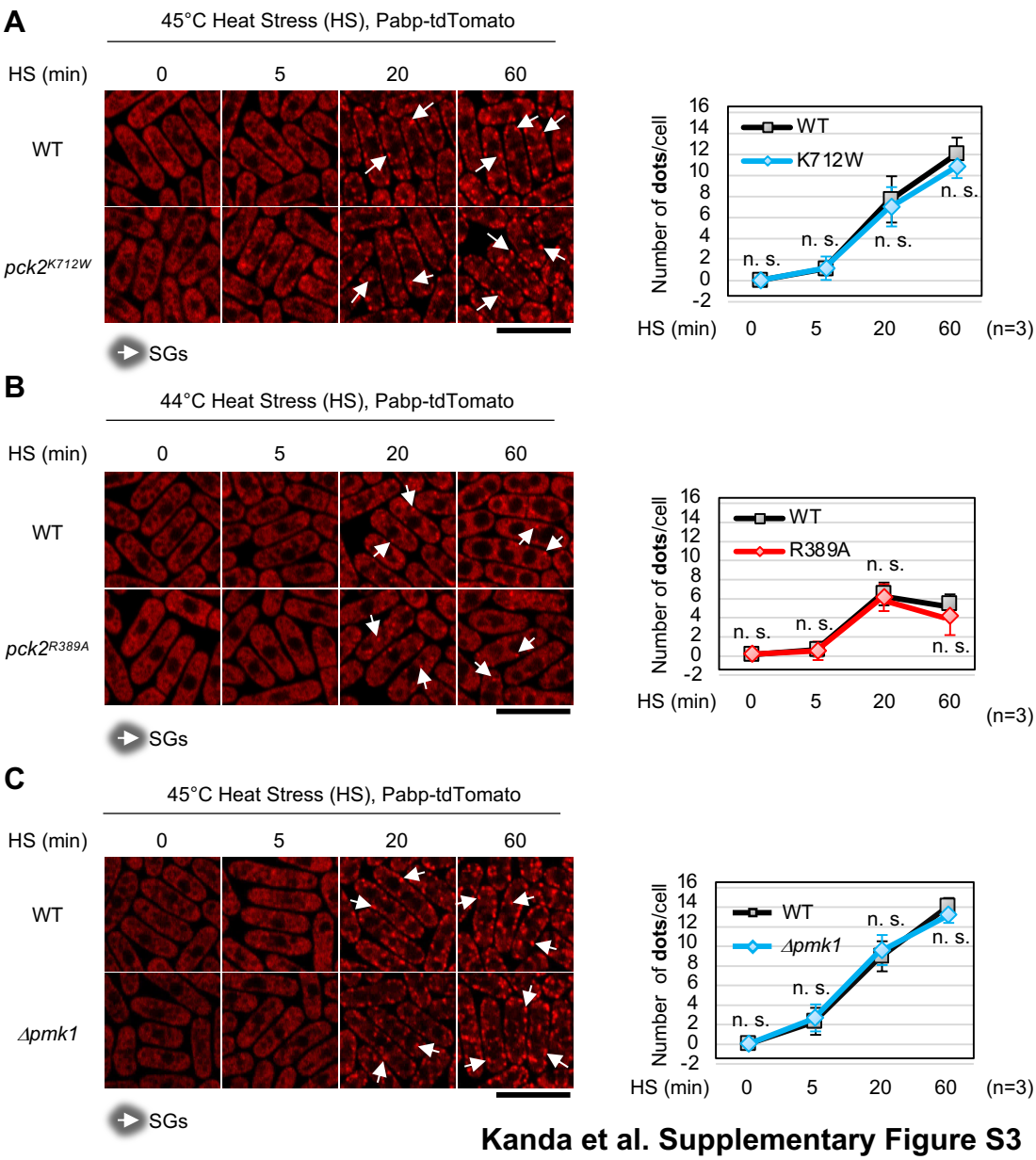

Kanda et al. Supplementary Figure S3

Figure S3. Pck2 K712W, Pck2 R389A, and Pmk1 deletion do not affect the Pabp-Positive SG assembly

(A, B, C) Left panel: Fluorescent images of the WT cells (A, B, C) or mutants (*pck2*^{K712W} (A), *pck2*^{R389A} (B), or *Dpmk1* (C)), expressing Pabp-tdTomato exposed to 45°C HS for the times indicated. Right panel: Quantification of the Pabp dots analyzed as in Figure 1B. Scale bars 10 µm. All graphs show mean ± s.d. (n=3). n.s.: not significant; significantly different from WT in each HS time point by Student's t-test; see Materials and Methods.

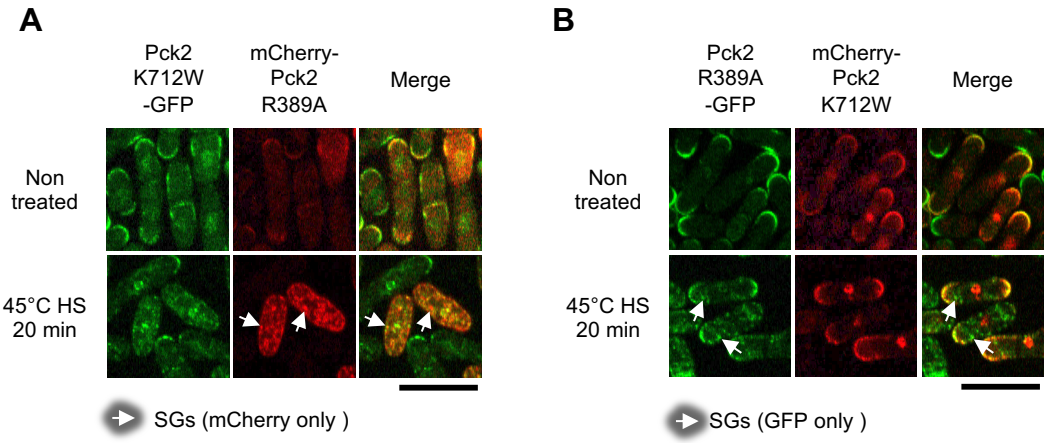

Kanda et al. Supplementary Figure S4

Figure S4. Visualization of the kinase-dead Pck2 and the constitutively active Pck2

(A) Wild-type cells expressing the endogenous Pck2 K712W-GFP and the exogenous mCherry-Pck2 R389A were grown in EMM at 27°C for 16 hr, then localization of Pck2 K712W-GFP and mCherry-Pck2 R389A were observed before (0 min) and after a shift to 45°C for 20 min. Arrows indicate the fluorescence of mCherry-Pck2 R389A dots (which do not co-localize with Pck2 K712W-GFP). Scale bars 10 µm. (B) Wild-type cells expressing the endogenous Pck2 R389A-GFP and the exogenous mCherry-Pck2 K712W were grown in EMM at 27°C for 16 hr, then localization of Pck2 R389A-GFP and mCherry-Pck2 K712W were observed before (0 min) and after a shift to 45°C for 20 min. Arrows indicate the fluorescence of Pck2 R389A-GFP dots (which do not co-locliaze with mCherry-Pck2 K712W). Scale bars 10 µm.

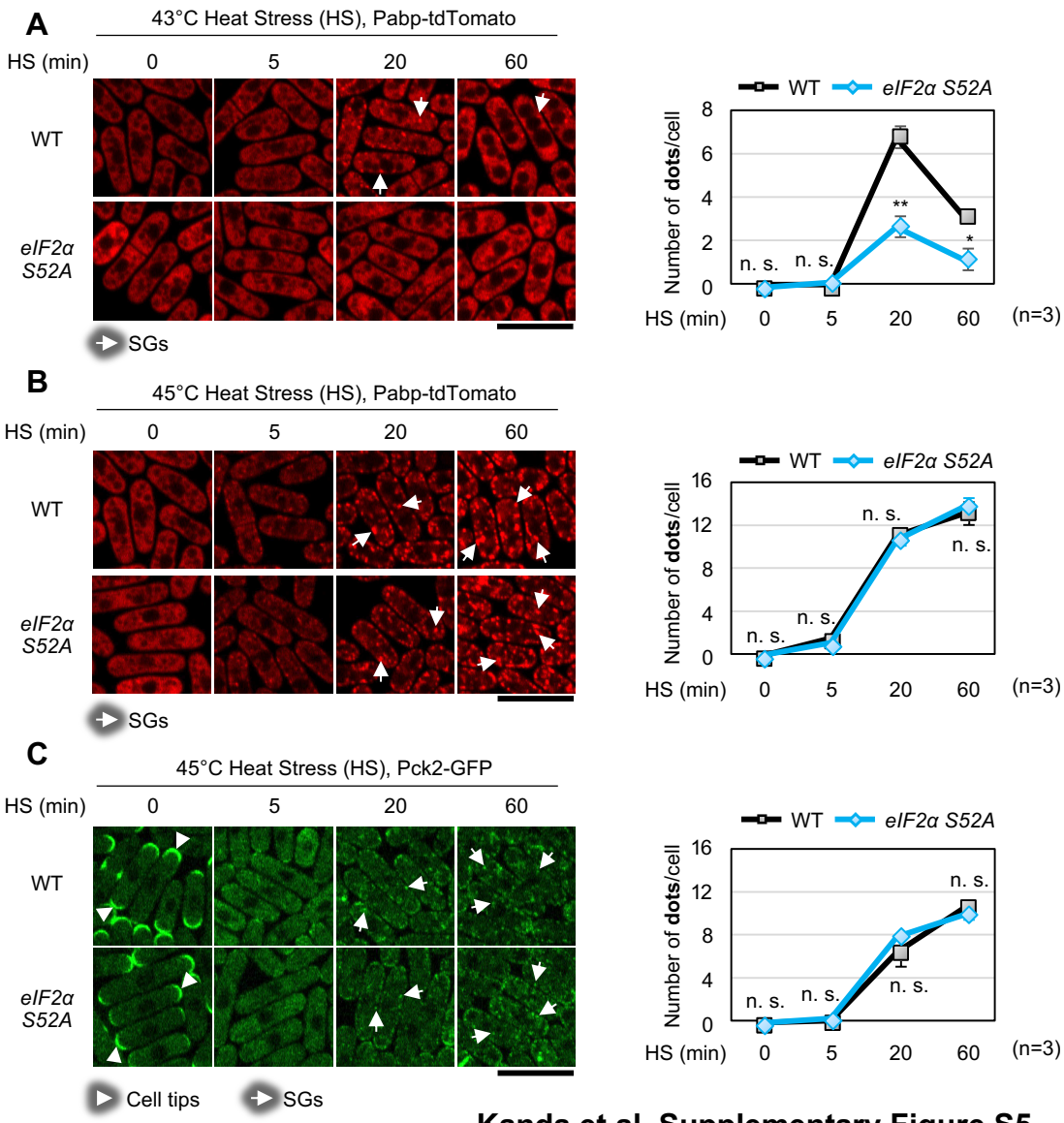

Kanda et al. Supplementary Figure S5

Figure S5. Pck2 translocation to SGs upon HS was independent of eIF2α phosphorylation

(A, B, C) Left panel: Fluorescent images of the WT or *eIF2α S52A* mutants, expressing Pabp-tdTomato (A, B) or Pck2-GFP (C) exposed to 43°C (A) or 45°C (B, C) HS for the times indicated. Right panel: Quantification of the Pabp dots or Pck2 dots analyzed as in Figure 1B. Scale bars 10 µm. All graphs show mean ± s.d. (n=3). *P<0.05, **P<0.01, n.s.: not significant; significantly different from WT in each HS time point by Student's t-test; see Materials and Methods.

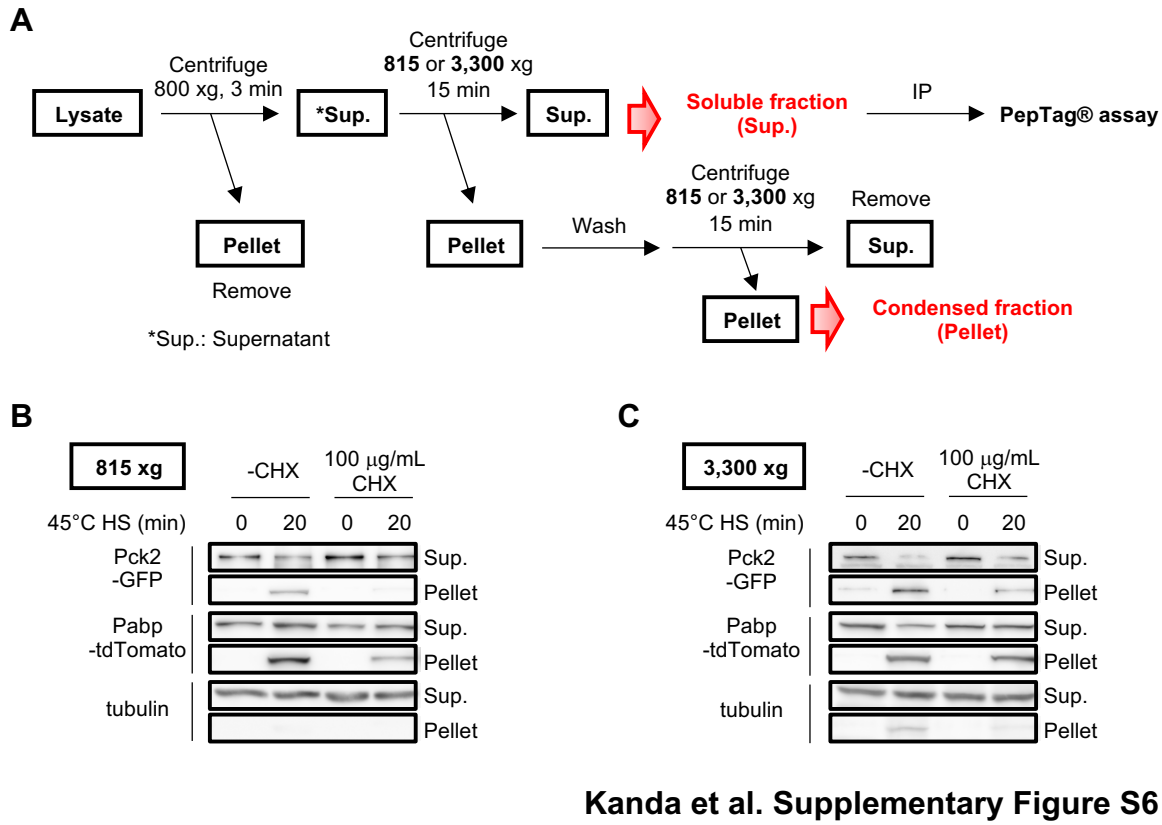

Kanda et al. Supplementary Figure S6

Figure S6. Preparation of stress granule enriched fraction from crude Cell lysate from fission yeast cells

(A) Scheme representation of the method for preparation of stress granule-containing condensed fraction and soluble fraction from crude cell lysate from fission yeast cells expressing Pck2-GFP and Pabp-tdTomato. (B, C) Samples obtained with a centrifuge at 815 ×g (B) or 3,300 ×g (C). Immunoblotting analysis showing the amount of Pck2-GFP, Pabp-tdTomato, and Tubulin from a soluble fraction (Sup.) or a SG-containing condensed fraction (Pellet) with or without the addition of CHX as is Figure 1E.

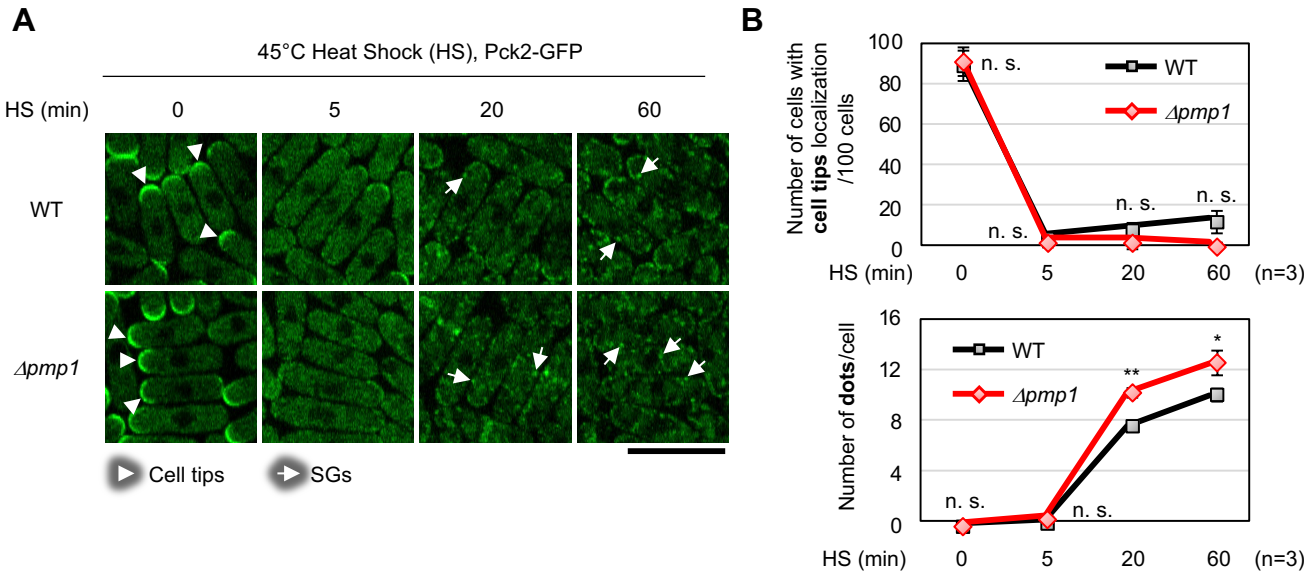

Kanda et al. Supplementary Figure S7

Figure S7. Deletion of Pmp1, a MAPK phosphatase for Pmk1, promotes Pck2 translocation to SGs

(A) Localizations of Pck2-GFP in WT or Pmp1 lacking cells after HS at 45°C for indicated time points. Arrowheads and arrows indicate the representative cell tips localization and foci of Pck2-GFP, respectively. Scale bars 10 µm. (B) Quantification of Pck2 localizations after HS at 45°C for indicated time points. Graphs show mean ± s.d. (n=3). *P<0.05, **P<0.01, n.s.: not significant; significantly different from WT in each HS time point by Student's t-test; see Materials and Methods.

***Schizosaccharomyces pombe* strain used in this study**		
Strain	Genotype	Reference
HM123	*h⁻ leu1-32*	Our stock
KP456	*h⁻ leu1-32 ura4-D18*	Our stock
KP843	*h⁻ leu1-32 ura4-D18 pmp1::ura4⁺*	Our stock
KP2118	*h⁻ leu1-32 ura4-D18 pmk1::KanMX6*	Our stock
SP385	*h⁻ leu1-32 ura4-D18 pmk1::ura4⁺*	Our stock
SP403	*h⁻ leu1-32 ura4-D18 pck2::ura4⁺*	Our stock
SP556	*h⁻ leu1-32 ura4-D18 pmk1⁺-GST::KanMX6*	Our stock
SP1657	*h⁻ leu1-32 ura4-D18 pck2⁺-GFP::ura4⁺*	Our stock
SP1704	*h⁻ leu1-32 pabp⁺-GFP::KanMX6*	Our stock
SP1705	*h⁻ leu1-32 ura4-D18 pabp⁺-GFP::KanMX6 nrd1::ura4⁺*	Our stock
SP1720	*h⁻ leu1-32 ura4-D18 ded1⁺-GFP::KanMX6 pck2⁺-GFP::ura4⁺*	Our stock
SP1934	*h⁻ leu1-32 ura4-D18 pck2⁺-GFP::ura4⁺ pabp⁺-tdTomato::HphMX6*	Our stock
SP2223	*h⁻ leu1-32 ded1⁺-GFP::KanMX6 pabp⁺-tdTomato::HphMX6*	Our stock
SP2231	*h⁻ leu1-32 pmk1⁺-GST::KanMX6*	Our stock
SP2350	*h⁻ leu1-32 ura4-D18 pck2⁺-GFP::ura4⁺ pmk1::ura4⁺*	Our stock
SP2451	*h⁻ leu1-32 ura4-D18 pmk1⁺-GST::KanMX6 pck1::ura4⁺*	Our stock
SP2704	*h⁻ leu1-32 ura4-D18 pmk1⁺-GST::KanMX6 pek1::ura4⁺*	Our stock
SP2982	*h⁻ leu1-32 pck2⁺-GFP::KanMX6*	This study
SP2983	*h⁻ leu1-32 pck2^{R389A}-GFP::KanMX6*	This study
SP2984	*h⁻ leu1-32 ura4-D18 pabp⁺-tdTomato::HphMX6 pmk1::ura4⁺*	This study
SP3055	*h⁻ leu1-32 pck2⁺-GFP::KanMX6 pmk1⁺-GST::KanMX6*	This study
SP3058	*h⁻ leu1-32 pck2^{K712W}-GFP::KanMX6*	This study
SP3067	*h⁻ leu1-32 pck2^{K712W}-GFP::KanMX6 pmk1⁺-GST::KanMX6*	This study
SP3077	*h⁻ leu1-32 pck2^{R389A}-GFP::KanMX6 pmk1::ura4⁺*	This study
SP3092	*h⁻ leu1-32 pck2^{R389A}-GFP::KanMX6 pmk1⁺-GST::KanMX6*	This study
SP3097	*h⁻ leu1-32 ura4-D18 pck2⁺-GFP::KanMX6 nrd1::ura4⁺*	This study
SP3100	*h⁻ leu1-32 ura4-D18 pmk1⁺-GST::KanMX6 nrd1::ura4⁺*	This study
SP3101	*h⁻ leu1-32 pck2⁺-GFP::KanMX6 pabp⁺-tdTomato::HphMX6*	This study
SP3102	*h⁻ leu1-32 pck2^{R389A}-GFP::KanMX6 pabp⁺-tdTomato::HphMX6*	This study
SP3103	*h⁻ leu1-32 pck2^{K712W}-GFP::KanMX6 pabp⁺-tdTomato::HphMX6*	This study
SP3111	*h⁻ leu1-32 pabp⁺-tdTomato::HphMX6*	This study
SP3117	*h⁻ leu1-32 ura4-D18 pck2⁺-GFP::KanMX6 eIF2α S52A::ura4⁺*	This study
SP3118	*h⁻ leu1-32 ura4-D18 pabp⁺-GFP::HphMX6 eIF2α S52A::ura4⁺*	This study
SP3166	*h⁻ leu1-32 pck2⁺-GFP::KanMX6 nrd1⁺-tdTomato::HphMX6*	This study
SP3166	*h⁻ leu1-32 ura4-D18 pck2⁺-GFP::KanMX6 pmp1::ura4⁺*	This study

Table S1

***Schizosaccharomyces pombe* primers used in this study**	
Gene	Primer
Pck2 K712W sense	5′-TGTATGCTATTTGGGTTTTGAAAAA-3′
Pck2 K712W antisense	5′-TTTTTCAAAACCCAAATAGCATACA-3′
Pck2 R389A sense	5′-GGATGCTGGCCTCGGAGCTCAAGGTGCTATCCG-3′
Pck2 R389A antisense	5′-CGGATAGCACCTTGAGCTCCGAGGCCAGCATCC-3′
Pck2 endogenous sense	5′-ATGGATATGATTGATGAGGC-3′
Pck2 endogenous antisense	5′-AAAAAGTCGAAATTAGAATAATTTATCAATGCAATGAAAGATTAAGAAAATGAGAGTAACTTTATGCTCAATTTAAGGTGGAATTCGAGCTCGTTTAAAC-3′

Antibodies used in this study			
Name	Source	Dilution	Remark
GFP	Abcam (ab1218)	1:1,000	Figure 2B, 2C, 4C, 7D, S6B, S6C for WB
GFP	Ma et al., 2006	1:250	Figure 2B, 2C, 4C, 7D for IP
GST	Ma et al., 2006	1:20,000	Figure 3A, 3B, 3C, 3D, 6B, 6D, S1A for WB
RFP	MBL (PM005)	1:1,000	Figure 7D, S6B, S6C for WB
Phospho Pmk1	Sugiura et al., 1999	1:20,000	Figure 3A, 3B, 3C, 3D, 6B, 6D for WB
α-tubulin	Sigma-Aldrich (T8203)	1:12,000	Figure 7D, S6B, S6C for WB
Rabbit-IgG	Cell signaling (7074)	1:4,000	Secondary antibody for GST, RFP, Phospho- Pmk1
Mouse-IgG	Cell signaling (7076)	1:4,000	Secondary antibody for GFP (Abcam), α-tubulin

Table S2

Number of **dots**/cell		
	45° C HS 20 min	45° C HS 60 min
Δ*pmk1*, Pck2 WT	2.68±0.40	6.96±0.75
Δ*pmk1*, Pck2 R389A	3.48±0.90	7.22±0.27
Significant differences	n. s.	n. s.

Table S3